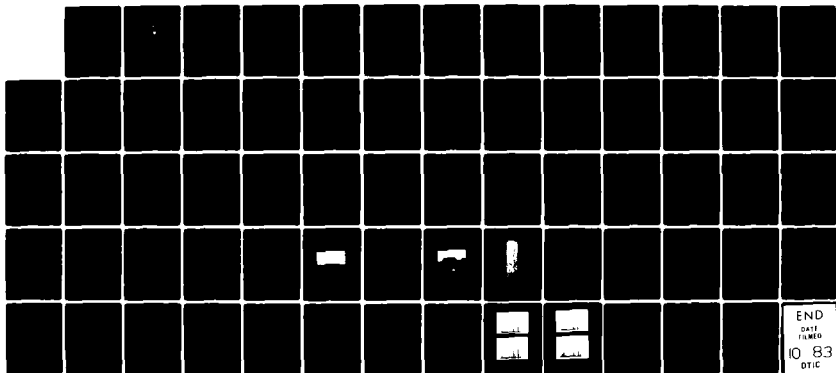


AN INVESTIGATION OF SUBSTRATE EFFECTS ON TYPE TWO HOT
CORROSION OF MARINE GAS TURBINE MATERIALS(U) NAVAL
POSTGRADUATE SCHOOL MONTEREY CA M J SHIMKO JUN 83

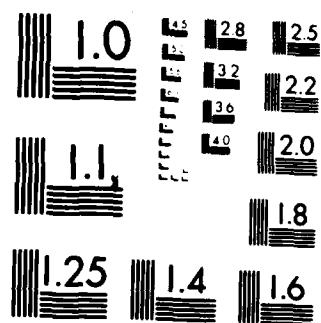
1/1

F/G 11/6

NL



END
DATE
FILMED
10 83
DTIC



MICROCOPY RESOLUTION TEST CHART
NATIONAL BUREAU OF STANDARDS-1963-A

AA A 132 833

27

NAVAL POSTGRADUATE SCHOOL

Monterey, California



DEPT. OF THE NAVY
JUN 23 1983

THESIS

AN INVESTIGATION OF SUBSTRATE EFFECTS
ON TYPE TWO HOT CORROSION OF MARINE
GAS TURBINE MATERIALS

by

Michael J. Shimko

June 1983

Thesis Advisor:

D.E. Peacock

Approved for public release; distribution unlimited

DTIC FILE COPY

83 09 20 150

UNCLASSIFIED

SECURITY CLASSIFICATION OF THIS PAGE (When Data Entered)

| REPORT DOCUMENTATION PAGE | | READ INSTRUCTIONS BEFORE COMPLETING FORM |
|---|-------------------------------------|--|
| 1. REPORT NUMBER | 2. GOVT ACCESSION NO. ADA132 833 | 3. RECIPIENT'S CATALOG NUMBER |
| 4. TITLE (and Subtitle) An Investigation of Substrate Effects on Type Two Hot Corrosion of Marine Gas Turbine Materials | | 5. TYPE OF REPORT & PERIOD COVERED Master's Thesis June 1983 |
| 7. AUTHOR(s) Michael J. Shimko | | 6. PERFORMING ORG. REPORT NUMBER |
| 8. PERFORMING ORGANIZATION NAME AND ADDRESS Naval Postgraduate School Monterey, California 93940 | | 9. CONTRACT OR GRANT NUMBER(s) |
| 11. CONTROLLING OFFICE NAME AND ADDRESS Naval Postgraduate School Monterey, California 93940 | | 10. PROGRAM ELEMENT, PROJECT, TASK AREA & WORK UNIT NUMBERS |
| 14. MONITORING AGENCY NAME & ADDRESS (if different from Controlling Office) | | 12. REPORT DATE June 1983 |
| | | 13. NUMBER OF PAGES 66 |
| | | 15. SECURITY CLASS. (of this report) |
| | | 15a. DECLASSIFICATION/DOWNGRADING SCHEDULE |
| 16. DISTRIBUTION STATEMENT (of this Report) Approved for public release, distribution unlimited | | |
| 17. DISTRIBUTION STATEMENT (of the abstract entered in Block 26, if different from Report) | | |
| 18. SUPPLEMENTARY NOTES | | |
| 19. KEY WORDS (Continue on reverse side if necessary and identify by block number) Marine Gas Turbines Hot Corrosion Substrate Effects Turbine Blade Coatings CoCrAlY | | |
| 20. ABSTRACT (Continue on reverse side if necessary and identify by block number) CoCrAlY coated Modifications of Rene 80 (a Ni base superalloy) were tested for resistance to Type Two (Low Temperature) Hot Corrosion. The effects of Ti and Hf in the substrate (normally 5.0% and 0.0% respectively) and the presence of a Pt underlayer were investigated. Certain trends were distinguishable from the data obtained. Titanium alone was found to be beneficial, Titanium in | | |

DD FORM 1 JAN 73 1473

EDITION OF 1 NOV 65 IS OBSOLETE
S/N 0102-LF-014-6601

UNCLASSIFIED

SECURITY CLASSIFICATION OF THIS PAGE (When Data Entered)

SECURITY CLASSIFICATION OF THIS PAGE (When Data Entered)

- conjunction with a platinum underlayer was found to be detrimental while platinum underlayers in conjunction with low titanium concentrations in the substrate were found to be beneficial. Hafnium had a noticeable, but irregular effect only on specimens with intermediate titanium concentrations. All the above effects were found to be diffusion related.

This study also made certain refinements to the NPS Hot Corrosion Test Program and direct correlation of data obtained from different runs is now justified.

Accession For

NTIS GRAB ☒

DTC TAB ☐

Unannounced ☐

Justification _____

Availability Codes
Availability Codes
Availability Codes

Print Sp. Unit

A

COPY 2

S. N 0102- LF- 014- 6601

SECURITY CLASSIFICATION OF THIS PAGE(When Data Entered)

Approved for public release; distribution unlimited.

An Investigation of Substrate Effects on
Type Two Hot Corrosion of Marine Gas Turbine Materials

by

Michael J. Shimko
Lieutenant, United States Navy
B.S., University of Maryland, 1977

Submitted in partial fulfillment of the
requirements for the degree of

MASTER OF SCIENCE IN MECHANICAL ENGINEERING

from the

NAVAL POSTGRADUATE SCHOOL
June 1983

Author:



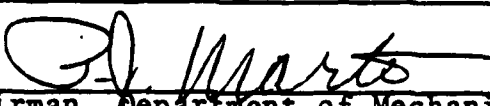
Approved by:




Thesis Advisor



Second Reader



Chairman, Department of Mechanical Engineering



Dean of Science and Engineering

ABSTRACT

CoCrAlY coated modifications of Rene 80 (a Ni base superalloy) were tested for resistance to Type Two (Low Temperature) Hot Corrosion. The effects of Ti and Hf in the substrate (normally 5.0% and 0.0% respectively) and the presence of a Pt underlayer were investigated.

Certain trends were distinguishable from the data obtained. Titanium alone was found to be beneficial, titanium in conjunction with a platinum underlayer was found to be detrimental while platinum underlayers in conjunction with low titanium concentrations in the substrate were found to be beneficial. Hafnium had a noticeable, but irregular effect only on specimens with intermediate titanium concentrations. All the above effects were found to be diffusion related.

This study also made certain refinements to the NPS Hot Corrosion Test Program and direct correlation of data obtained from different runs is now justified.

TABLE OF CONTENTS

| | | |
|------|---|----|
| I. | INTRODUCTION | 10 |
| A. | HISTORICAL | 10 |
| 1. | Naval Experience with the Gas Turbine . . . | 10 |
| 2. | Superalloys | 12 |
| 3. | Coatings | 13 |
| B. | HOT CORROSION | 16 |
| 1. | Hot Corrosion Testing | 18 |
| 2. | Previous Research | 21 |
| C. | OBJECTIVES | 22 |
| II. | PROCEDURE | 23 |
| III. | DISCUSSION/RESULTS | 26 |
| A. | SUBSTRATE EFFECTS | 28 |
| IV. | CONCLUSIONS AND RECOMMENDATIONS | 36 |
| | APPENDIX A: TABLES | 38 |
| | APPENDIX B: FIGURES | 43 |
| | LIST OF REFERENCES | 64 |
| | INITIAL DISTRIBUTION LIST | 66 |

LIST OF TABLES

| | | |
|------|---|----|
| I. | Nominal Chemical Composition of Rene' 80 and | |
| | BC-21 | 38 |
| II. | Test Parameters | 39 |
| III. | Listing and Results of Duplicate Pins | 40 |
| IV. | Listing of Samples Tested - Substrate Study | 41 |
| V. | Corrosion Results - Substrate Study | 42 |

LIST OF FIGURES

| | | |
|------|---|----|
| B.1 | Relative Temperature and Pressure Profile of a Marine Gas Turbine Engine | 43 |
| B.2 | Simplified Drawing of the Electron Beam Physical Vapor Deposition (EB-PVD) Process | 44 |
| B.3 | Typical CoCrAlY (BC-21) Coating on Rene' 80 | 45 |
| B.4 | Type 2 (Low Temperature) Hot Corrosion Simplified Schematic | 46 |
| B.5 | Typical Type 2 Hot Corrosion in CoCrAlY (BC-21) Coating | 47 |
| B.6 | Typical Type 2 Hot Corrosion on BC-21 Coating - Macrophoto (enlarged 7.5 x) | 48 |
| B.7 | Cross Section of a Tube Furnace | 49 |
| B.8 | Schematic Illustration of the Substrate/Coating Diffusion Process | 50 |
| B.9 | Schematic Illustration of the Method of Using High Magnification Spectrochemical Analysis for Diffusion Study | 51 |
| B.10 | The Effect of SO ₂ Flow Rate on Type 2 Hot Corrosion of BC-21 Coated Rene' 80 | 52 |
| B.11 | Type 2 Hot Corrosion Behavior of BC-21 Coated Rene' 80 Modifications, Effect of Titanium | 54 |
| B.12 | Type 2 Hot Corrosion Behavior of BC-21 Coated Rene' 80 Modifications, Effect of Platinum | 57 |
| B.13 | Type 2 Hot Corrosion Behavior of BC-21 Coated Rene' 80 Modifications, Effect of Hafnium | 59 |

| | |
|---|----|
| B.14 Chemical Spectrums of Center of BC-21 Coated and Corroded Rene' 80 (5% Ti Modification) | 62 |
| B.15 Chemical Spectrums of BC-21 Coating on Corroded Rene' 80 (5% Ti Modification) with Platinum Underlayer | 63 |

ACKNOWLEDGMENT

The author would like to thank the staff of the Mechanical Engineering Department for their timely and efficient assistance and in particular to Adjunct Professor David E. Peacock, Adjunct Professor David H. Boone, and Mr. Tom Kellogg whose enthusiasm, help, and encouragement were instrumental in the completion of this thesis.

A special thanks to my loving wife, Donna, and our recently arrived Jackelyn for their inspiration, support, and sacrifice throughout my stay at the Naval Postgraduate School.

I. INTRODUCTION

A. HISTORICAL

1. Naval Experience with the Gas Turbine

The United States Navy is currently pursuing one of the most ambitious shipbuilding programs since the end of World War II. In the last 10 years all new combatants have relied on either nuclear power or the gas turbine as their source of propulsive power.

The Engine chosen for development and use by the Navy was the CF6/TF39 aircraft engine used on the C5 Transport aircraft. The marinized version of this engine has been designated the LM2500. The LM2500 is currently used in or scheduled for use in 30 DD-963 Spruance Class Destroyers, 4 DDG-993 Kidd Class Guided Missile Destroyers, 50 FFG-7 Perry Class Guided Missile Frigates, the CG47 Tichondoroga Class Guided Missile Cruisers, the DDG-51 Class Guided Missile Destroyer, numerous hydrofoils and Surface Effect Ships, and a large number of commercial industrial and marine applications as well.

Over the years gas turbine efficiency has grown through increased technology and design achievements but has been always limited by the high temperature materials used within the gas turbine, specifically within the high pressure turbine area which immediately follows the combustor assembly.

A simplified schematic and relative temperature and pressure profile of the LM2500 is shown in Figure B.1.

The United States first use of the gas turbine was on the GTS CALLAGAN in 1967 when extensive testing of several versions of gas turbines was undertaken. In 1973 the Navy committed itself to the LM2500 engine. The first tests of the LM2500 involved primarily long term high power runs, and in 1971 the initial DD power cycle testing was begun. These tests were thought to provide the most arduous operating environment for initial evaluation. The lifetime of the critical turbine blades was found to be approximately 7000 hours. The limiting factor was Hot Corrosion of the blade coating which was known to occur at temperatures over 850°C.

In 1973, partly in response to the oil embargo, a test cycle which reduced the average speed to 19 knots was started as a fuel conservation measure. Since at low power the maximum temperature of the gas turbine is less than for high power, it was predicted that the lifetimes of the critical gas turbine blading would be extended in this operating environment (this follows from classical arrhenius kinetics considerations). Unexpectedly, the blading lifetime was significantly reduced to less than 5000 hours. This was the Navy's first experience with Low Temperature Hot Corrosion (often referred to as Type 2 Hot Corrosion) {Ref. 1}. Subsequent changes in the operating cycle of CALLAGAN further

reduced the time spent at full power from 60 to 18%, and the resulting turbine blade lifetimes diminished even further. Since these initial tests, blade lifetimes have been increased by improvements in intake air filtration systems to better remove sea salt spray. However Type 2 Hot Corrosion is still limiting blade life to 5000 hours, compared to 7000 hours if Type 2 Hot Corrosion were not a factor.

Given the need for significant amounts of time spent at low power operations while maintaining the capability to run at full power as mission needs dictate, Type 2 Hot Corrosion will continue to be a factor in the future.

2. Superalloys

In the development of the gas turbine, material selection of the critical high temperature and pressure components has been based primarily on mechanical behavior criteria (creep resistance, high temperature strength, etc.), and use of protective coatings to provide additional resistance to the corrosive environment.

The superalloys are a class of iron, nickel and cobalt based alloys with various other elements added to achieve high temperature creep resistance, high temperature tensile strength, resistance to mechanical and thermal fatigue, as well as resistance to oxidation and hot corrosion [Ref. 2].

In nickel based superalloys, desired high temperature properties are obtained by the formation of a coherent second phase, gamma prime ($\text{Ni}_3(\text{Al}, \text{Ti})$) in a continuous

nickel matrix, gamma {Ref. 3} . Although both phases have fcc structures, slightly different lattice parameters result in coherency strains which results in an increment of strengthening. In general, the more gamma prime phase present, while still maintaining a continuous gamma phase, the better the mechanical properties.

An increase in the amount of gamma prime can be achieved by a reduction in chromium content and an increase in the amount of titanium and/or aluminum {Ref. 4 } . Since chromium also enhances grain boundary strengthening, this results in one of many tradeoffs.

The effect of high chromium then is a lower strength at high temperatures compared with alloys with a lower chromium content but with other solid-solution strengthening elements such as tungsten and molybdenum. Chromium and aluminum both form protective oxides which result in improved oxidation and hot corrosion resistance {Ref. 5} .

3. Coatings

The alloy additions which confer the desired high temperature strength of superalloys generally lower their resistance to hot corrosion, oxidation, and thermal fatigue {Ref. 6}. Surface coatings are used to improve environmental resistance. This is usually accomplished by the formation of a protective oxide such as Al_2O_3 and/or Cr_2O_3 .

The primary basis for selecting a protective coating is its inherent environmental resistance (i.e., its ability

to form the required protective oxide). However, since it has been demonstrated {Ref. 7} that the coating and substrate can influence each other, the selection process requires that the coating and substrate be considered together as an integral system. However, the possible removal of the coating by wear or FOD (foreign object damage) and the difficulty of coating some interior surfaces of gas turbine airfoils requires that the uncoated basemetal should provide a minimal degree of corrosion resistance. A first consideration in this respect is similar or at least compatible mechanical properties. For this reason current coatings in use today are either Aluminide Diffusional Coatings or Metallic Overlay Coatings.

Aluminide diffusional coatings are formed by diffusion aluminum into the surface of the substrate and converting them into an intermetallic compound. The resulting coating consists of an inner reaction-diffusion zone and one or two outer zones of intermetallic compounds of the metal aluminide type {Ref. 6}. Upon oxidation exposure, an aluminum oxide film forms on the surface and is the primary barrier against further oxidation. This oxide is reformed as required by the underlying aluminide.

Aluminide coatings are brittle at low and intermediate temperatures, and provide only moderate Hot Corrosion resistance when compared with most overlay coatings. Duplex coatings (Modified Aluminide Coatings) have been developed

which have shown enhanced corrosion resistance. This has been accomplished by the addition of elements such as chromium, or noble metals such as platinum to the aluminide coating.

The limitations of the aluminide coatings: brittleness, moderate corrosion resistance, and a strong substrate dependence have led to the development of the Metallic Overlay Coatings. These coatings are often of the MCrAlY type (where M = Fe, Ni, and/or Co) and are primarily applied by the Physical Vapor Deposition (PVD) process. A simplified schematic of one form of PVD process, the electron beam PVD (the process used for the coating of samples for this study) is shown in Figure B.2. These coatings consist of two phases; a brittle aluminide phase in a ductile, chromium rich solid-solution matrix. A typical overlay coating, BC-21, is shown in Figure B.3. This class of coatings contain from 4 to 13% Al, 18 to 40% Cr, and 0.1 to 0.5% Y with the balance either Co and/or Ni. The aluminum and chromium are protective oxide formers and the yttrium enhances oxide adhesion. The ability to vary the composition of these coatings for specific applications is a significant advantage over aluminide coatings. The composition of BC-21 is given in Table I (along with the composition of Rene' 80, a Ni based superalloy). BC-21 is the coating on the first and second stage turbine blades of the LM2500. It has a relatively high Cr content, 20 to 24%, which enhances Hot Corrosion resistance [Ref. 8]. This necessitates a lower Al content to maintain sufficient ductility. The beneficial

effects of platinum in aluminide coatings has led to testing of Overlay Coatings containing platinum and also of Overlay coatings applied over platinum underlayers.

A third type of coating currently being studied is the Ceramic Coating. This offers the dual advantage of good corrosion resistance and high thermal resistance. This could allow increased turbine inlet temperatures and/or reduce cooling air requirements. Ceramic coatings have not yet been developed with sufficiently compatible mechanical properties for full airfoils and are not yet in commercial use {Ref. 9}.

B. HOT CORROSION

The surface degradation of marine gas turbine materials can be the result of several corrosion mechanisms. These may act singly, independently, or in combination. The known mechanisms are: oxidation, catastrophic oxidation, high temperature hot corrosion, and low temperature hot corrosion. Specific morphologies have been identified that occur by some of the mechanisms above. Type 1 morphology is characteristic of the attack under conditions of high temperature hot corrosion on CoCrAlY type coatings. Type 2 morphology occurs in CoCrAlY type coatings under low temperature hot corrosion conditions. Type 3 morphology seems to occur under a combination of high temperature and low temperature hot corrosion conditions and/or in environments with a high SO_3 partial pressure. Based on these morphologies, the two main

forms of hot corrosion are now more correctly termed Type 1 (high temperature) Hot Corrosion, and Type 2 (low temperature) Hot Corrosion. Their shorthand abbreviations, HTHC and LTHC are commonly used and will be used throughout this study.

Type 1 Hot Corrosion has been known since the mid-1950's. It is associated with gas turbines used in jet aircraft which are usually run at high power levels. HTHC occurs in a temperature range above about 850°C. It requires a molten salt (Na_2SO_4) film and a specific range of partial pressures of O_2 and SO_3 and results in the dissolution of the protective oxide and the formation of a characteristic zone of aluminum depletion in advance of the corrosion front {Ref. 10}. Since Na_2SO_4 has a melting point of 886°C Hot Corrosion was not expected to be a problem at temperatures much below this. In 1975, observations on the GTS CALLAGAN showed otherwise {Ref. 1}.

Type 2 Hot Corrosion attacks CoCrAlY coatings without preference to phase. It also requires a molten salt, but in this case it is an eutectic mixture (Na_2SO_4 and MSO_4) which can have melting points as low as 575°C. LTHC also requires gaseous SO_3 , the partial pressure of which has been shown to be critical to LTHC attack {Ref. 11}. In more detail, Cobalt oxides formed on the coating react with gaseous SO_3 to form CoSO_4 which is absorbed by the Na_2SO_4 in the molten salt mixture. As the CoSO_4 dissolves, the melting point of the mixture is further reduced, until

at 50% CoSO_4 an eutectic point at 560°C is reached {Ref. 12}. As the alloy begins to react with the molten salts, oxygen is removed from the molten salt phase and partial pressure gradients of O_2 and SO_3 are developed across the liquid, and SO_3 thus supplies the oxygen to react with elements in the alloy.

Aluminum and sulfite ions react in areas of low oxygen partial pressure and aluminum is selectively removed from the coating and precipitated as aluminum oxide in areas of high oxygen partial pressure. This process is classic acidic fluxing and results in the severe pitting attack associated with LTHC. Figure B.4 shows a simplified schematic of the mechanism described above, Figure B.5 shows a photomicrograph of a typical example of the pitting attack, and Figure B.6 shows a macrophoto of typical Type 2 Hot Corrosion. Despite the lower temperature at which it occurs (compared to Type 1 attack), LTHC is generally more severe. This is partially due to the good wetting ability of the molten eutectic salt mixture which enables LTHC to attack the coating at microscopic imperfections in the protective oxide layer.

1. Hot Corrosion Testing

Hot Corrosion Testing in the laboratory involves the use of accelerated tests in order to duplicate the corrosion of possibly 5000 hours of turbine usage in a reproducible manner. Many form of testing are available

today, and in general the better they match actual gas turbine conditions, the higher the cost, complexity, and required time. Pressurized burner rigs provide the closest laboratory simulation of actual turbine conditions {Ref. 6} by allowing control of gas pressures, velocities, composition, and temperature. Pressures up to 15 atm. and velocities up to mach 1.0 have been utilized to minimize the time required for corrosive attack.

A less costly test method is the simple burner rig. This test apparatus consists essentially of a burner for the fuel, a combustion chamber, and a test chamber for the samples. Contaminants (salts, SO_2 , etc.) may be injected into the test chamber, mixed with the air supply, or mixed with the fuel supply (prior to combustion). Abnormally high levels of contaminants may be employed to obtain measurable attack within a few hundred hours, but for more consistent results, burner rig exposures of up to 5000 hours (approximately 7 months) have been recommended {Ref. 6}.

A third type of Hot Corrosion testing involves the use of a laboratory furnace. In this type of test samples are placed in the furnace at the desired temperature and exposed to a flowing gas mixture of air and SO_2 . In addition, prior to this, the samples are sprayed with a salt solution ensuring a given level of salt film on the sample surface. In this way, the initiation phase of LTHC (the presence of a molten salt film) is essentially eliminated and a greatly

accelerated test is obtained. This is the type of test used in the Naval Postgraduate School Hot Corrosion Program. A simplified schematic of the tube furnace used at NPS is shown in Figure B.7. The total time required to produce typical Type 2 morphology is only 60 hours, and has given results comparable to those obtained using the more expensive and time consuming burner rig tests {Ref. 13}.

A possible shortcoming of such an accelerated test method is that the relatively short time involved at high temperatures (60 hours) allows for very limited inter-diffusion between the substrate and coating, whereas in a typical gas turbine blade lifetime of 5000 hours, there is ample time for diffusion. The possible inter-diffusion of elements that may take place is illustrated in Figure B.8. A process devised to more closely simulate the actual life of a turbine blade involves what is called pre-exposure. In pre-exposure, samples are exposed to a time/temperature environment that has been predicted to allow for the diffusion that would take occur in 40% of a turbine blade lifetime {Ref. 14}. To minimize oxidation of the coating during pre-exposure, samples are vacuum sealed in quartz tubes. Further details of the pre-exposure process are described under PROCEDURES. Following pre-exposure, the samples are furnace tested as described above.

2. Previous Research

The Hot Corrosion research program at the Naval Postgraduate School has been ongoing since 1979 and has focused primarily on substrate effects on Type 2 Hot Corrosion resistance. The following highlights the results of this program to date. Hafnium has been reported to be beneficial to LTHC resistance, but only up to some optimal (0.4 to 2.0%) concentration, {Ref. 15}. Newberry {Ref. 16} conducted testing of uncoated superalloys, which included a study of the effect of Hafnium on the LTHC resistance of IN738. Pre-exposure was first used in 1981 and resulted in evidence of a detrimental effect on LTHC of inter-diffusion between the substrate and coating for some systems {Ref. 14}. Jurey {Ref. 17} carried out a more extensive investigation of pre-exposure and reported on the overall degrading effects of pre-exposure on LTHC resistance. He also reported that a platinum underlayer could be beneficial to LTHC resistance (the effect was sensitive to thickness), and observed that the maximum penetration measured on corroded test samples was very sensitive to pre-existing flaws, leaders, etc. In 1981, McGowen designed, tested, and validated the parameters used to perform Type 1 (high temperature) Hot Corrosion Testing. {Ref. 18}

C. OBJECTIVES

A variable that has been difficult to control in the Hot Corrosion Program at the Naval Postgraduate School has been the SO_2 content of the furnace atmosphere. The low flow rate required (10 ml/min) is difficult to maintain by most needle valves and is very sensitive to line pressure. The SO_2 flow rate has been observed to drop in this study from 15 ml/min to 5 ml/min in 5 hours. Type 2 Hot Corrosion resistance has been shown to vary significantly with change in SO_2 flow rates at NPS (Ref. 13 and 16). For this reason one or two control pins were inserted in each furnace run of this study to determine if variations in SO_2 flow rate (and/or possibly other parameters) were affecting the corrosive conditions of the test. In addition, 4 samples in Run MS1 were re-tested in Run MS7 as a basis for determining what kind of a modifying factor, if any, should be applied to the results of a given run to allow comparison of the results from different runs. Finally, an electronic flow controller has been installed, enabling accurate and continuous monitoring of the SO_2 flow rate.

The objectives of this study were to determine the effects of varying the amounts of titanium and hafnium present in the alloy substrate and the presence or absence of both a thick and thin platinum underlayer on the Type 2 Hot Corrosion behavior of BC-21 coated Rene' 80. Hot Corrosion testing was performed both with and without pre-exposure.

II. PROCEDURE

Test specimens consisted of nominally 0.6 cm. diameter pins of modified Rene' 80 superalloy. The modification consisted of varying the titanium and hafnium content of the alloy (Rene' 80 normally contains 5.0% Ti, and 0.0% Hf), see Table IV. One pin of each composition was coated with the CoCrAl_y coating BC-21 using the EB-PVD method. One pin of each composition received a platinum flash prior to application of a BC-21 coating, and one pin of each composition received a 5-6 μ m platinum undercoating (this thickness has been shown to be optimal in other coating/substrate systems) prior to application of a BC-21 coating. The platinum was applied by electrodeposition.

The procedures described below and listed in Table II were developed and validated by Busch (Ref. 13).

Each test piece, a cylindrical pin nominally 2.0 cm in length by 0.6 cm in diameter, was visually inspected for defects and its length and diameter accurately measured. The specimen was then inserted in an oven at 150°C for 20 minutes, after which it was cooled, weighed on an analytical balance, and replaced in the oven for an additional 20 minutes. After removal from the furnace the second time, and while still hot, the specimen was sprayed with a Na₂SO₄ 40 mole % Mg₂SO₄ solution and then returned to the furnace

for 15 minutes. It was then removed, cooled, and weighed. This was repeated until a weight gain representing an average of 1 mg salt per cm^2 of surface area was obtained.

After salting, the specimen was placed in a holder together with other similarly prepared specimens and inserted into a resistance type tube furnace as shown in Figure B.7. Once brought to the desired temperature (704°C), the specimens were exposed to a flowing gas mixture consisting of dry air (flow rate of 2000 ml/min) and 0.5% SO_2 . This flow rate has been determined to give a gas velocity of 1 cm/sec {Ref. 17}. The specimens were exposed to this corrosive environment for 20 hours, after which they were removed from the furnace, cooled to room temperature, visually inspected, weighed, and resalted as described above. Three 20 hour cycles were used for a total exposure of 60 hours.

Upon completion of the 60 hours, the specimens were examined visually and photographed (Figure B.6 shows a closeup of a typical sample). The pins were then sectioned in three places and prepared for microscopic examination using standard metallographic procedures.

Depth of corrosion measurements were taken every 20 degrees around a face. The pit like nature of the attack allows the location of the original surface of the coating to be accurately determined. Recorded was the mean penetration, (typically the average of 54 readings), standard deviation of the mean, the maximum penetration, and the average coating thickness observed. The

pre-exposure treatment given to some specimens prior to LTHC testing consisted of sealing in evacuated quartz tubes to minimize surface degradation and heat treating in an oven at 875°C for 200 hours.

In addition to optical microscopy selected samples were examined using a Scanning Electron Microscope. Backscatter images, spectrums, and line traces were made in an attempt to determine the concentrations of the elements at different locations in the coatings and substrates, particularly in those specimens subjected to the pre-exposure treatment. Since line traces and backscatter images proved to be of little use in this regard (due to poor resolution of minor constituent changes), spectrums were taken at 5000X at three locations in the coating: at the coating/substrate interface, at the center of the coating, and just under the corrosion front near the top of the coating, as shown schematically in Figure B.9. From these spectrums moderate changes in elemental concentrations were distinguishable.

As previously mentioned, at least one control pin was inserted in each run to allow direct comparison of test conditions between runs. An electronic flow controller was installed on 28 March 1983 and its calibration verified with a new rotometer. Run MS6 was made using this to control the SO₂ flow rate. A final Run, MS7 was made containing several identical pins to check the reproducibility of the results.

III. DISCUSSION/RESULTS

Table III lists the specimens tested which were re-tested in various runs. They are listed simply as "Type 1, Type 2, etc." to prevent any significance being placed on their compositions and were chosen originally for their availability. Also included in Table III are the actual corrosion results (the mean and maximum penetration), and the adjusted mean penetration (to be explained). Figure B.10a and b is the graphical presentation of this data. It illustrates the variation in corrosive conditions between furnace runs. Similar variation of results between different runs has been seen in a review of previous studies {Ref. 16}, although the nature and cause of these variations were not known.

Upon installation of the electronic flow controller for SO_2 flow rate control, it was observed that the original rotometer read approximately 100 ml/min when the new controlled read 10 ml/min. The original rotometer (believed to have been in use since 1979) was replaced with a new rotometer, which agreed closely with the electronic controller. This is evidence that the rotometer previously in use had been giving incorrect flow rate readings (probably due to the corrosive nature of the SO_2 gas) which probably began gradually such that no individual researcher was aware of a change in the actual flow rate. By 1983, when this

study was begun, a reading of 10 ml/min from the original rotometer resulted in an actual SO₂ flow rate of only 2 ml/min, which was too small a flow to be easily controlled by the needle valve arrangement installed at that time. This led to the observation that the SO₂ flow rate tended to drop off with time (but seldom in a predictable manner). After the first run or two, it was possible to get a crude "feel" for how to best maintain a roughly constant SO₂ flow rate, and this is somewhat reflected by the improved reproducibility between runs MS4 and MS5. It is recommended that the SO₂ flow rate be continually monitored by two different methods (the electronic flow controller and a new rotometer), in order that any slight change in SO₂ flow is detected early and can be corrected.

Figure B.10a also shows the high degree of consistency obtained between runs MS6 and MS7 (the electronic flow controller was installed prior to run MS6). This supports the claim that variation in the SO₂ flow rate was primarily responsible for inconsistencies observed in past furnace runs and also illustrates the high degree of consistency obtained within a given run (note samples MS7-2 thru MS7-9).

Due to the possibility of inconsistencies in corrosive conditions between runs the use of a modifying factor was thought to be useful. With run MS6 as a baseline and using control pin type 1 (since this was the most common control used), a modifying factor was developed using the following formula:

$$MF = \text{Mean}(6) / \text{Mean}(x)$$

where MF = Modifying Factor

Mean(6) = Mean penetration of the control
pin on run MS6

Mean(x) = Mean Penetration of the control pin
in run MSx

The mean penetration data for each run was then multiplied by the modifying factor for the run. This "adjusted data" is shown graphically in Figure B.10b and shows fair correlation of data from different runs.

Since the maximum penetration of a sample has been noted to be very sensitive to the presence of pre-existing flaws and leaders, and since it represents only a single area of localized attack, mean penetration (typically the average of over 50 measurements) is used for comparison and evaluation. This is consistent with methods used previously at NPS. For this reason only the mean penetration data has been adjusted, the maximum penetration has been included for completeness only.

A. SUBSTRATE EFFECTS

Table IV lists the samples that were tested as part of this study. As mentioned previously the concentration of Titanium and Hafnium were varied as was the presence of and thickness of a platinum underlayer. Each type of sample was tested with and without pre-exposure. The sample abbreviations listed were designed to indicate to the reader the approximate

titanium concentration, whether or not hafnium was present, if a platinum underlayer was present (and if so, a thin platinum flash or a thicker, 5-6um underlayer), and also if the sample was pre-exposed. Also included are the original serial numbers for possible use by future researchers reviewing this study.

Table V lists the samples by their abbreviations, along with the mean and maximum penetration, as mentioned previously, the mean penetration data has been adjusted by the use of modifying factors, and this is the data used in evaluation of results.

The mean penetration data in Table V are presented graphically in Figures B.11, B.12, and B.13. Each figure contains 4 or 6 individual graphs, and presents the entire data of Table V, but each in a slightly different manner in order to highlight specific trends. All the figures plot the tabulated corrosion behavior as a function of titanium concentration for ease of correlation. In Figure B.11 there are 6 plots, each for a specific platinum underlayer and hafnium combination, with a comparison of with/without pre-exposure evident on each individual plot. This set primarily illustrates the effect of titanium. Figure B.12 contains 4 plots, each for a specific combination of hafnium and pre-exposure, and primarily illustrates the effect of platinum underlayers. Figure B.13 contains 6 plots, each for a specific combination of platinum underlayer and pre-exposure,

and best illustrates the hafnium effect. Due to the number of variables involved (which results in 36 different types of specimens), the attempt was made to highlight trends rather than the possible significance of a single specimen performing differently from another. Therefore a relative ranking of all specimens tested is not included or discussed. Finally, the data of most significance is for the specimens that were pre-exposed since this better reflects corrosion behavior well into the life of a turbine blade. The data for specimens not pre-exposed was used primarily as an aid in explaining why certain results are obtained (i.e., if a trend is diffusion related, then it would show an effect due to pre-exposure). Therefore unless otherwise stated, hereafter any trends or other observations noted are assumed to be made for pre-exposed samples.

Figure B.11a and b show a decrease in mean penetration as Ti content is increased. This trend is either not as distinct or not observed in the samples which were not pre-exposed. Observations previously made on the effect of titanium were usually the result of the testing of different substrates (i.e., IN738 and Rene' 80) from which a distinct effect of titanium was difficult to discover {Ref. 14}.

It was noted here that Ti was beneficial to LTHC resistance only if the time/temperature history of the sample was sufficient to allow for diffusion. In particular, the mean penetration of the following samples from Figure B.11a:

(2-0-0), (5-0-0), (2-0-0-E), (5-0-0-E) distinctly indicates the advantage of allowing diffusion to take place for both low (2.0%) and high (5.0%) Ti content.

High magnification (5000X) x-ray backscatter spectrums of (5-0-0) and (5-0-0-E) were made. While the spectrums obtained are by no means quantitative, they can give an indication as to whether diffusion is occurring. The spectrums obtained from the center of the coating of these samples are shown in Figure B.14. The only difference is the presence of a small peak due to Ni in (5-0-0-E), indicating slight diffusion of Ni into the coating. While titanium was not observed in either case, this does not preclude the possible diffusion of titanium. This is because spectrums taken well into the substrate indicate that 5% titanium is roughly the minimum concentration required to be distinguishable by SEM backscatter analysis. Additionally, Katz (Ref. 19) has reported on the presence of titanium at the surface of BC-21 coated Rene'80. Ni was not observed in the spectrums taken at the outer edge of the coating on either sample. A backscatter dot-map and line probe for chromium was made on (5-0-0-E). These both indicated an enhanced concentration of chromium at the coating/substrate interface. This was not observed on (5-H-0-E). Since only a small number of samples were subjected to examination with the Scanning Electron Microscope, it is not known if this enhanced chromium concentration at the interface is present in other

samples, or if it results from the coating process, rather than as a result of high temperature exposure. At this time, the chromium concentration noted has not been observed in other samples.

When platinum is present, Figures B.11e and f indicate titanium is detrimental to LTHC resistance. In particular, sample (2-0-PP-E) performed much better than (5-0-PP-E). Figure B.11e and f also dramatically show that without pre-exposure this trend is reversed. SEM spectrum analysis was performed on (5-0-PP) and (5-0-PP-E) and the spectrums from the center of the coatings are included in Figure B.15. The spectrum for (5-0-PP) shows no platinum and no nickel. On (5-0-PP-E), a definite platinum peak is observed, as well as nickel. The chromium and cobalt contents at the coating center of (5-0-PP-E) are possibly lower than those at the coating center of (5-0-PP).

Figure B.12b and d indicate that platinum (if the titanium content is high) is detrimental to LTHC resistance. Comparison of data on Figures B.12a and b show this effect to be reversed when pre-exposure is not performed. However, Figure B.12b and d show slight benefit of adding platinum underlayers to samples with only 2% titanium. SEM back-scatter analysis was not performed on samples (2-0-PP) and (2-0-PP-E), but it is thought that platinum has diffused into the coating in sample (2-0-PP-E), based on the diffusion noted in (5-0-PP-E). Previous studies by Clark (Ref. 20) have

shown the beneficial effect of platinum underlayers on CoCrAl_y coatings.

A possible explanation of these observations is as follows. Without a platinum underlayer, and given the opportunity for diffusion, titanium diffuses outward into the coating where it produces a beneficial effect. Therefore, the higher the titanium concentration in the substrate, the better the LTHC resistance.

When platinum underlayers are applied and an opportunity for diffusion (i.e., during exposure) exists the platinum underlayer can improve LTHC resistance. However, the titanium in the substrate may react with the platinum. At the 2% titanium level, titanium cannot diffuse due to this interaction, but there is enough excess platinum (notably in the 5-6 μ m thick underlayer) to allow sufficient platinum to diffuse outward to be of benefit.

At the 3.5% titanium level, the sample without a platinum underlayer exhibits better LTHC resistance due to the additional diffusion of titanium. The sample with platinum underlayers shows little change, since the titanium remains at the interface. At the 5% titanium level, however, there is sufficient titanium for some titanium to diffuse through the platinum underlayer into the coating, where it combines with the platinum that has already diffused outward, forming compounds that prove to be detrimental to LTHC resistance.

This last suggestion is supported by two observations:
1) sample (5-0-PP-E) performed significantly worse than (5-0-0-E), (2-0-PP-E) and (5-0-PP), which again indicates that platinum and titanium in combination have a detrimental effect, and 2) significant diffusion of platinum into the coating has been noted in (5-0-PP-E).

Detailed microprobe analysis must be performed to determine if indeed titanium is diffusing into the coating in (5-0-PP-E), and (5-0-0-E), and if, and what, compounds are being formed. Additionally, since the lowest level of titanium for this study was 2%, testing of samples with 0% titanium, with and without a platinum underlayer, would more clearly indicate the role of platinum in LTHC resistance.

The effects of hafnium on LTHC resistance proved to be difficult to discern. Figure B.13 was included to present these results. Comparing Figure B.13b, d, and f, hafnium seems to have a noticeable (but inconsistent) effect on the samples with 3.5% Ti (with a platinum flash hafnium was beneficial, but with 5-6 um platinum hafnium was detrimental). At the 2% and 5% Ti levels, hafnium has no noticeable effect. On samples that were not pre-exposed (Figure B.13a, c, and e) the reverse seems to be true. Hafnium has a noticeable (but again inconsistent) effect at 2% and 5% Ti, and a negligible effect on the 3.5% Ti samples.

Optical examination was unable to distinguish any differences in the coating structure or corrosion attack due

to the presence of hafnium. Previous studies, mainly on the nickel based alloy IN738 which contains 3.4% titanium, have shown an optimum level of hafnium to exist, which ranged from 0.4% to 2.0%, depending on the study. The 1.2 to 1.5% hafnium level chosen for this investigation is within this range. Although evidence is lacking, it is possible that the normally beneficial effect of hafnium is being influenced by the interactions suggested above.

IV. CONCLUSIONS AND RECOMMENDATIONS

Based on the data, tables, and figures discussed, the following conclusions can be made:

1. The presence of titanium in the substrate (in the absence of a platinum underlayer) is beneficial to LTHC resistance, provided that the time/temperature environment allows for interdiffusion between the substrate and coating.
2. The combined presence of titanium in the substrate and a platinum underlayer are detrimental to LTHC resistance, again if inter-diffusion between the substrate and coating occurs.
3. Platinum underlayers are detrimental to LTHC resistance if the titanium content of the substrate is relatively high (5.0%), again if inter-diffusion occurs.
4. Hafnium has a definite, but inconsistent effect on LTHC resistance when intermediate levels of titanium (3.5%) are present in the substrate; this effect again depends upon inter-diffusion.
5. Hot Corrosion testing conducted prior to the installation of the electronic SO₂ flow controller that required correlation of data collected by separate furnace runs should be reviewed to determine if direct comparison between runs was justified, or if modifying factors should be applied to the results.

6. For Hot Corrosion testing conducted subsequent to the installation of the electronic SO₂ flow controller direct correlation of data obtained from different runs is justified.

The above conclusions and the previous discussion lead to the following list of recommendations:

1. Conduct a detailed, quantitative microprobe analysis of selected specimens used in this study in an attempt to determine more precisely diffusional changes that are occurring in order to better explain the behavior and effects noted above.

2. Test samples with 0.0% titanium, and also 10.0% titanium (with and without platinum underlayers) to obtain additional data to support or refute the suggested explanations of the effects observed in the study.

3. Perform a similar study on BC-21 coated IN738, an alternative substrate alloy. This would require a study of the effect of hafnium and platinum only.

4. Review previous NPS research for possible intra-run comparisons that may not be justified, and, if possible, re-evaluate the data obtained using modifying factors and, based on this adjusted data, re-examine the results previously obtained.

APPENDIX A

TABLES

TABLE I
Nominal Chemical Composition of Rene' 80 and BC-21

| | Ni | Co | Cr | Al | Y | Ti | W | Mo |
|----------|------|------|------|------|-----|-----|-----|-----|
| Rene' 80 | Bal. | 9.5 | 14.0 | 3.0 | --- | 5.0 | 4.0 | 4.0 |
| BC-21 | --- | Bal. | 23.0 | 12.0 | 0.3 | --- | --- | --- |

TABLE II

TEST PARAMETERS

Pre-Exposure:

preliminary - vacume sealed in quartz tubes
temperature - 875°C
time - 200 hours

Type 2 Hot Corrosion

air, source - laboratory air
flow rate - 2000 ml/min
SO₂, source - bottled gas
flow rate - 10 ml/min (0.5%)
salting, type - Na₂SO₄ 40 mole% MgSO₄
amount - 1.0 mg/cm²
temperature - 704°C
thermal cycle - 20 hours
number of cycles - 3
total time - 60 hours

TABLE III

LISTING AND RESULTS OF DUPLICATE PINS

| Sample Group Nr. | Original Serial Nr. (Run Nr. - Pin Nr.) | Mean Penetration (μm) | Max. Penetration (μm) | Adjusted Mean Penetration (μm) |
|---------------------|---|--|--|---|
| 1 | MS1-7 | 7.9 | 76.2 | 23.7 |
| 1 | MS4-13 | 17.4 | 137.2 | 23.7 |
| 1 | MS5-12 | 20.2 | 127.0 | 23.7 |
| 1 | MS6-14 | 23.7 | 132.0 | -- |
| 1 | MS7-2 | 24.9 | 139.1 | -- |
| 1 | MS7-3 | 22.5 | 111.8 | -- |
| 1 | MS7-4 | 25.6 | 190.5 | -- |
| 1 | MS7-5 | 21.1 | 146.1 | -- |
| 1 | MS7-6 | 24.1 | 171.0 | -- |
| 1 | MS7-7 | 20.9 | 203.2 | -- |
| 1 | MS7-8 | 23.6 | 139.1 | -- |
| 1 | MS7-9 | 25.2 | 185.6 | -- |
| 2 | MS4-7 | 4.6 | 66.0 | 6.2 |
| 2 | MS6-12 | 5.6 | 76.2 | 6.5 |
| 3 | MS1-2 | 7.9 | 76.2 | 23.6 |
| 3 | MS7-13 | 26.1 | 190.5 | -- |
| 4 | MS1-8 | 8.6 | 91.4 | 25.9 |
| 4 | MS7-14 | 21.6 | 157.5 | -- |
| 5 | MS1-5 | 10.4 | 94.0 | 31.2 |
| 5 | MS7-15 | 22.1 | 167.6 | -- |

TABLE IV

LISTING OF SAMPLES TESTED - SUBSTRATE STUDY

| Sample Abbreviation | Composition (%Ti, %Hf, Pt, Exp.) | | | | Original Serial Nr. (Run Nr. - Pin Nr.) |
|------------------------|-------------------------------------|-----|-------------|-----|--|
| (2-0-0) | 2.0 | 0 | 0 | no | MS1-9 |
| (2-0-p) | 2.0 | 0 | flash | no | MS5-13 |
| (2-0-PP) | 2.0 | 0 | 5-6 μ m | no | MS1-3 |
| (2-H-0) | 2.0 | 1.5 | 0 | no | MS1-8 |
| (2-H-p) | 2.0 | 1.5 | flash | no | MS5-9 |
| (2-H-PP) | 2.0 | 1.5 | 5-6 μ m | no | MS1-2 |
| | | | | | |
| (3.5-0-0) | 3.5 | 0 | 0 | no | MS5-6 |
| (3.5-0-p) | 3.6 | 0 | flash | no | MS5-11 |
| (3.5-0-PP) | 3.6 | 0 | 5-6 μ m | no | MS5-8 |
| (3.5-H-0) | 3.5 | 1.5 | 0 | no | MS5-7 |
| (3.5-H-p) | 3.5 | 1.5 | flash | no | MS5-2 |
| (3.5-H-PP) | 3.5 | 1.5 | 5-6 μ m | no | MS5-1 |
| | | | | | |
| (5-0-0) | 5.0 | 0 | 0 | no | MS1-6 |
| (5-0-p) | 5.0 | 0 | flash | no | MS5-5 |
| (5-0-PP) | 5.0 | 0 | 5-6 μ m | no | MS5-10 |
| (5-H-0) | 5.0 | 1.2 | 0 | no | MS1-5 |
| (5-H-p) | 5.0 | 1.2 | flash | no | MS5-4 |
| (5-H-PP) | 5.0 | 1.2 | 5-6 μ m | no | MS5-3 |
| | | | | | |
| (2-0-0-E) | 2.0 | 0 | 0 | yes | MS4-9 |
| (2-0-p-E) | 2.0 | 0 | flash | yes | MS6-13 |
| (2-0-PP-E) | 2.0 | 0 | 5-6 μ m | yes | MS4-3 |
| (2-H-0-E) | 2.0 | 1.5 | 0 | yes | MS4-8 |
| (2-H-p-E) | 2.0 | 1.5 | flash | yes | MS6-9 |
| (2-H-PP-E) | 2.0 | 1.5 | 5-6 μ m | yes | MS4-2 |
| | | | | | |
| (3.5-0-0-E) | 3.5 | 0 | 0 | yes | MS6-6 |
| (3.5-0-p-E) | 3.6 | 0 | flash | yes | MS6-11 |
| (3.5-0-PP-E) | 3.6 | 0 | 5-6 μ m | yes | MS6-8 |
| (3.5-H-0-E) | 3.5 | 1.5 | 0 | yes | MS6-7 |
| (3.5-H-p-E) | 3.5 | 1.5 | flash | yes | MS6-2 |
| (3.5-H-PP-E) | 3.5 | 1.5 | 5-6 μ m | yes | MS6-1 |
| | | | | | |
| (5-0-0-E) | 5.0 | 0 | 0 | yes | MS4-6 |
| (5-0-p-E) | 5.0 | 0 | flash | yes | MS6-5 |
| (5-0-PP-E) | 5.0 | 0 | 5-6 μ m | yes | MS6-10 |
| (5-H-0-E) | 5.0 | 1.2 | 0 | yes | MS4-5 |
| (5-H-p-E) | 5.0 | 1.2 | flash | yes | MS6-4 |
| (5-H-PP-E) | 5.0 | 1.2 | 5-6 μ m | yes | MS6-3 |

TABLE V

CORROSION RESULTS - SUBSTRATE STUDY

| Sample Abbreviation | Mean Penetration (μm) | Max. Penetration (μm) |
|------------------------|---------------------------------------|---------------------------------------|
| (2-0-0) | 37.6 | 76.2 |
| (2-0-p) | 18.0 | 106.7 |
| (2-0-PP) | 35.8 | 86.4 |
| (2-H-0) | 24.4 | 101.6 |
| (2-H-p) | 27.2 | 167.6 |
| (2-H-PP) | 22.6 | 76.2 |
| | | |
| (3.5-0-0) | 24.4 | 91.4 |
| (3.5-0-p) | 21.3 | 101.6 |
| (3.5-0-PP) | 17.8 | 193.0 |
| (3.5-H-0) | 21.3 | 190.5 |
| (3.5-H-p) | 22.6 | 132.1 |
| (3.5-H-PP) | 20.8 | 101.6 |
| | | |
| (5-0-0) | 26.4 | 81.3 |
| (5-0-p) | 13.0 | 88.9 |
| (5-0-PP) | 15.0 | 66.0 |
| (5-H-0) | 31.2 | 66.0 |
| (5-H-p) | 23.4 | 381.0 |
| (5-H-PP) | 20.6 | 81.3 |
| | | |
| (2-0-0-E) | 15.7 | 81.3 |
| (2-0-p-E) | 18.8 | 89.9 |
| (2-0-PP-E) | 8.6 | 81.3 |
| (2-H-0-E) | 17.8 | 81.3 |
| (2-H-p-E) | 15.0 | 152.4 |
| (2-H-PP-E) | 14.0 | 279.4 |
| | | |
| (3.5-0-0-E) | 11.7 | 177.8 |
| (3.5-0-p-E) | 15.5 | 76.2 |
| (3.5-0-PP-E) | 9.7 | 177.8 |
| (3.5-H-0-E) | 9.1 | 132.1 |
| (3.5-H-p-E) | 5.6 | 127.0 |
| (3.5-H-PP-E) | 23.6 | 116.8 |
| | | |
| (5-0-0-E) | 6.4 | 71.1 |
| (5-0-p-E) | 18.3 | 101.6 |
| (5-0-PP-E) | 22.9 | 111.8 |
| (5-H-0-E) | 7.6 | 96.5 |
| (5-H-p-E) | 22.9 | 127.0 |
| (5-H-PP-E) | 24.1 | 127.0 |

APPENDIX B

FIGURES

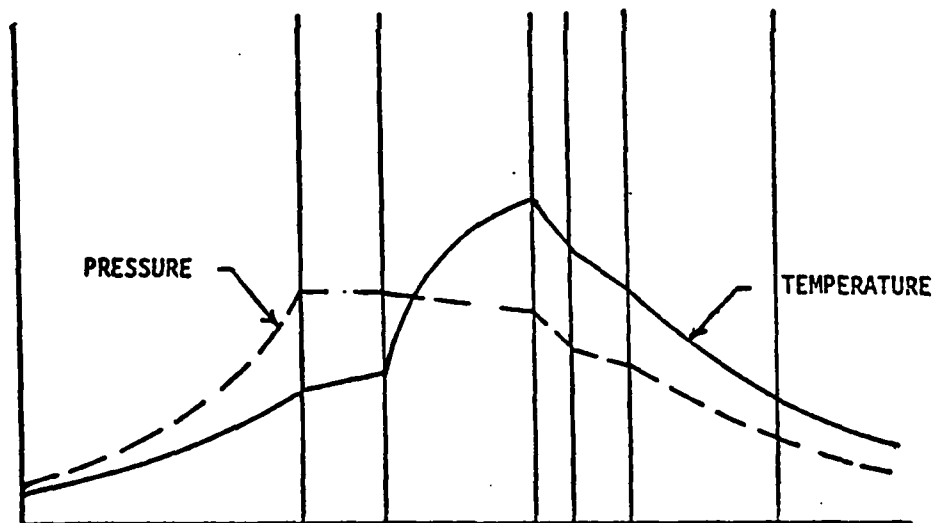
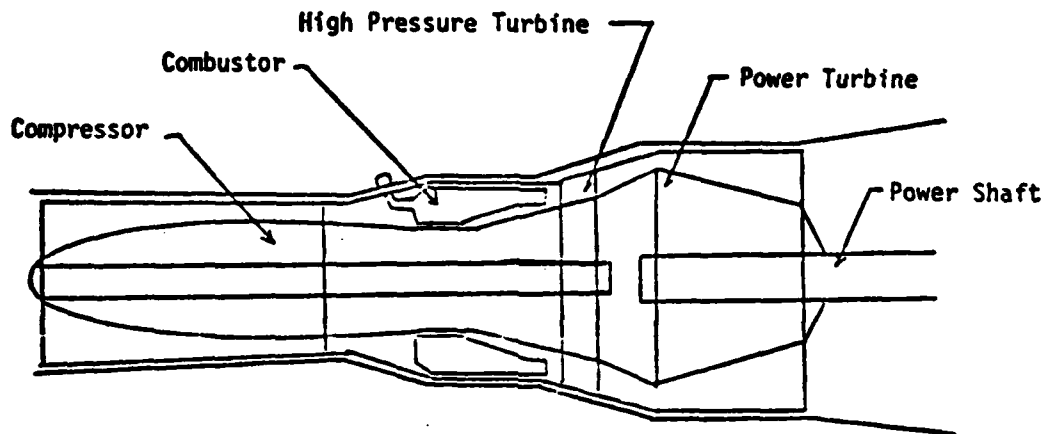


Figure B.1 Relative Temperature and Pressure Profile of a Marine Gas Turbine Engine

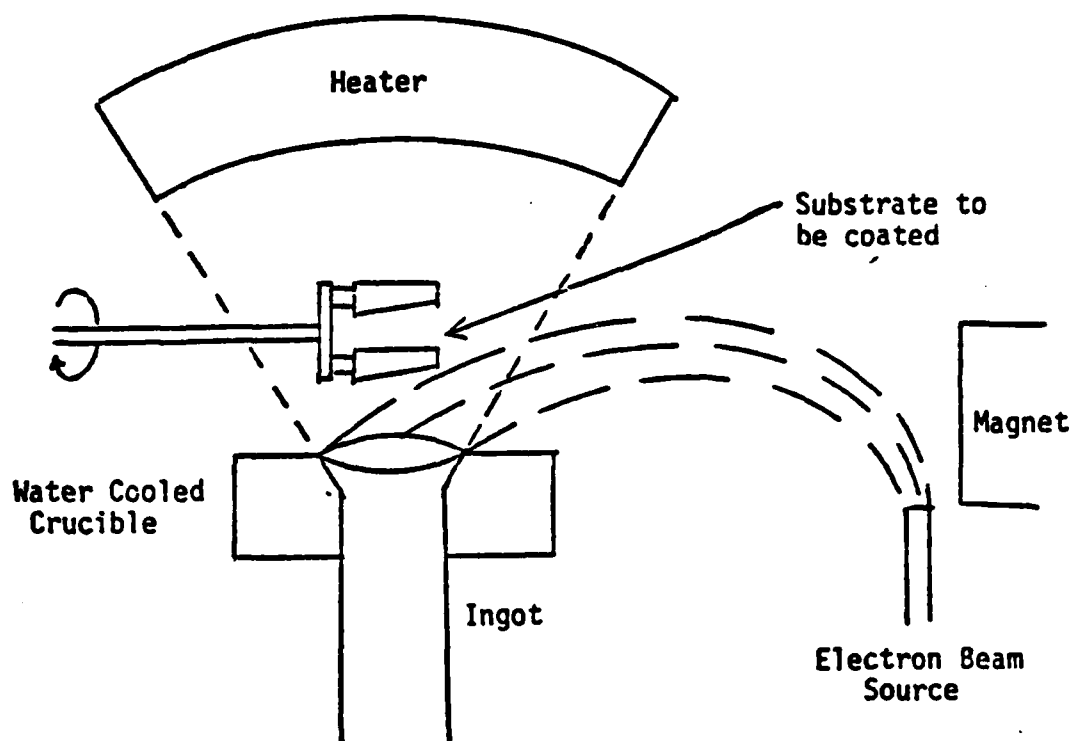
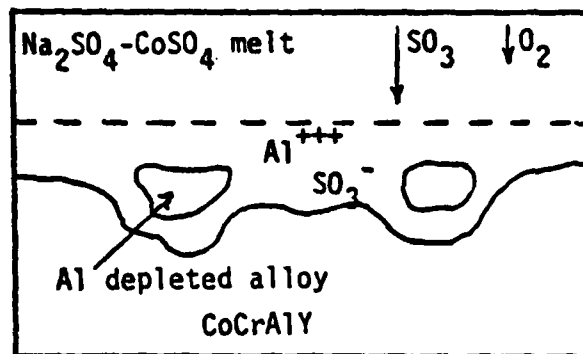


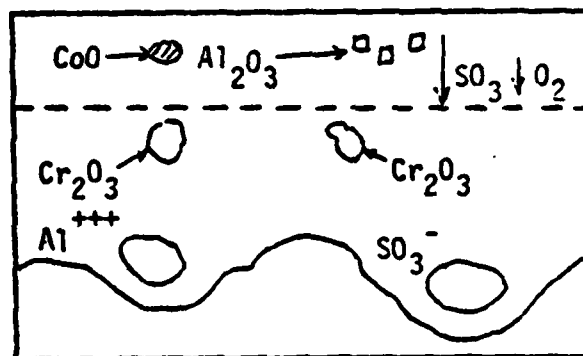
Figure B.2 Simplified Drawing of the Electron Beam Physical Vapor Deposition (EB-PVD) Process



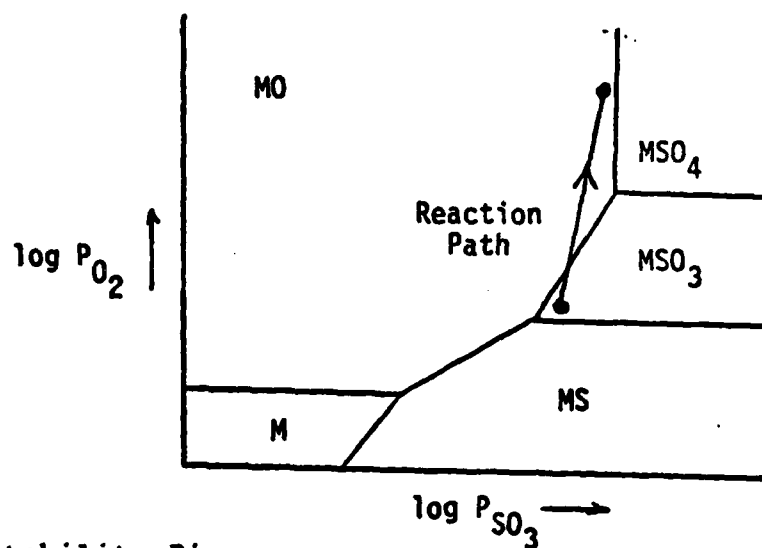
Figure B.3 Typical CoCrAlY (BC-21) Coating on Rene' 80



(a) Onset of Type 2 Attack



(b) Corrosion Front Continues to Dissolve Coating



(c) Stability Diagram

Figure B.4 Type 2 (Low Temperature) Hot Corrosion.
Simplified Schematic

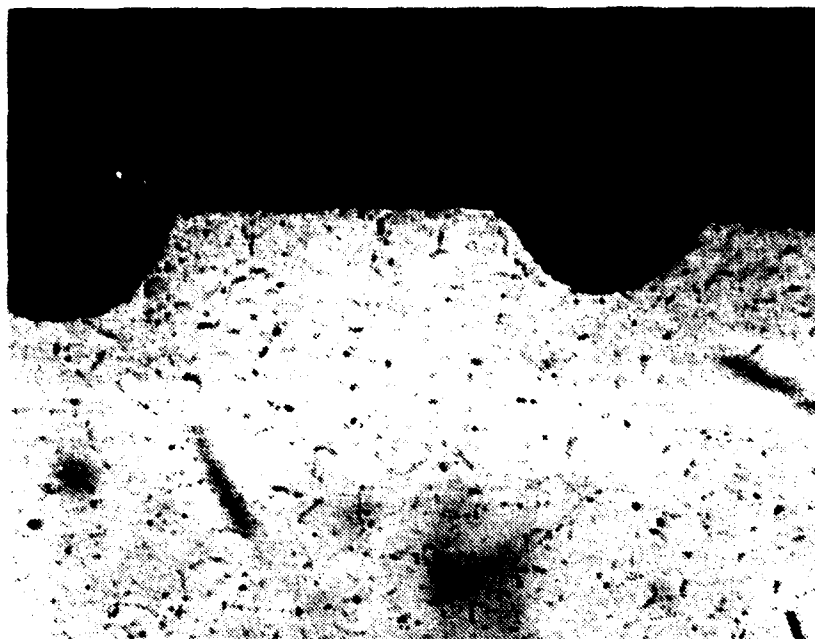


Figure B.5 Typical Type 2 Hot Corrosion in CoCrAlY (BC-21)
Coating

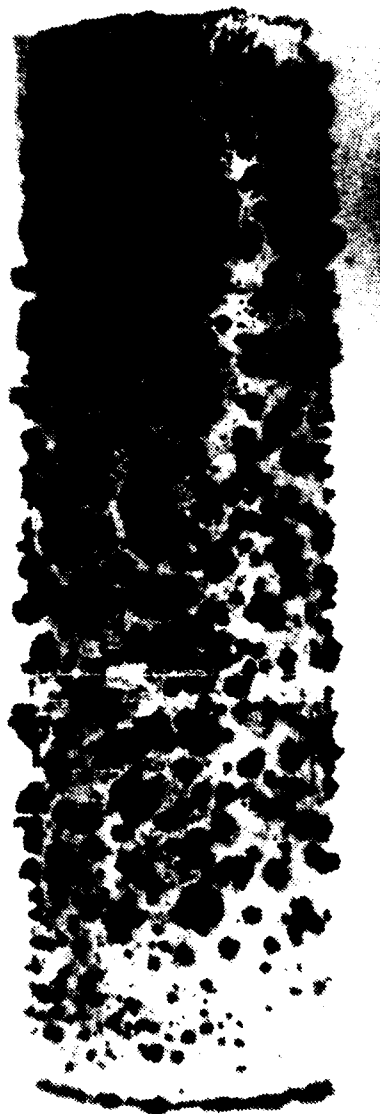


Figure B.6 Typical Type 2 Hot Corrosion on BC-21 Coating -
Macrophoto (enlarged 7.5 x)

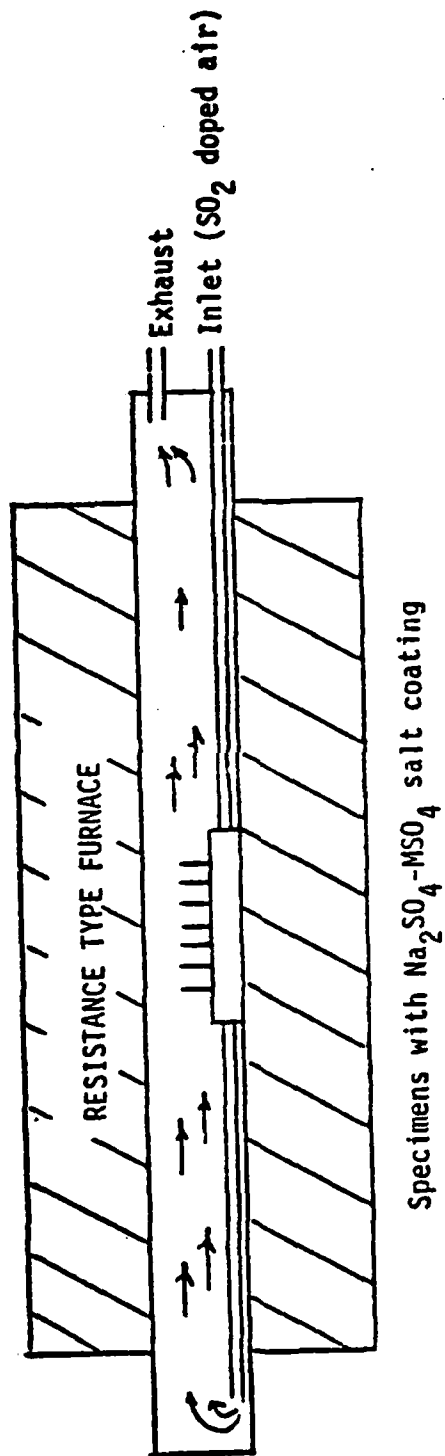
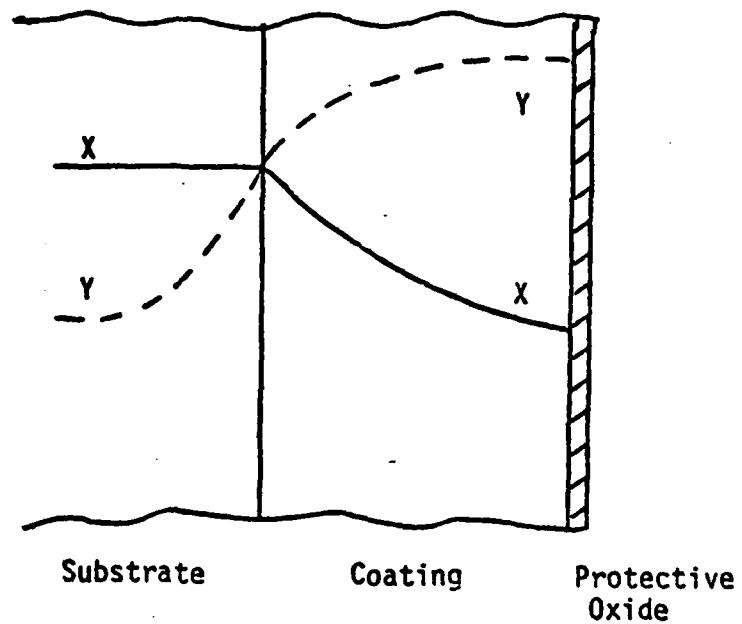


Figure B.7 Cross Section of a Tube Furnace



Typical X elements

Ni
W
Mo
Ti
Hf
Pt

Typical Y elements

Al
Cr
Co
Y
Pt

Figure B.8 - Schematic Illustration of the Substrate/Coating Diffusion Process

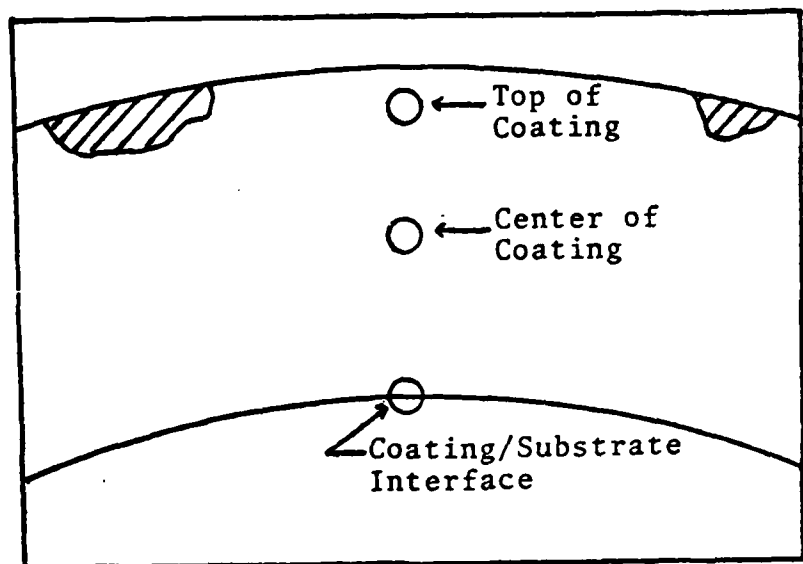
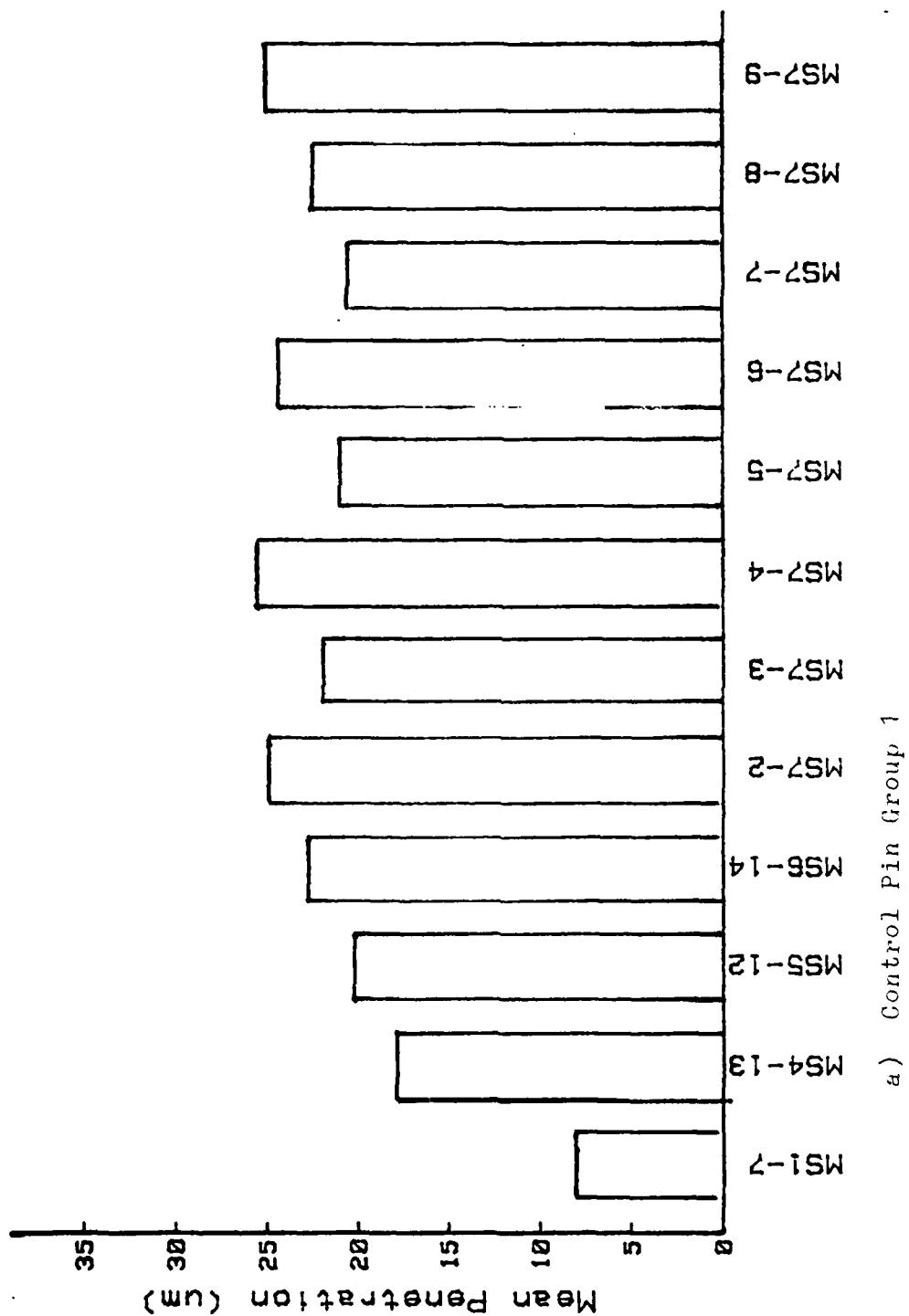
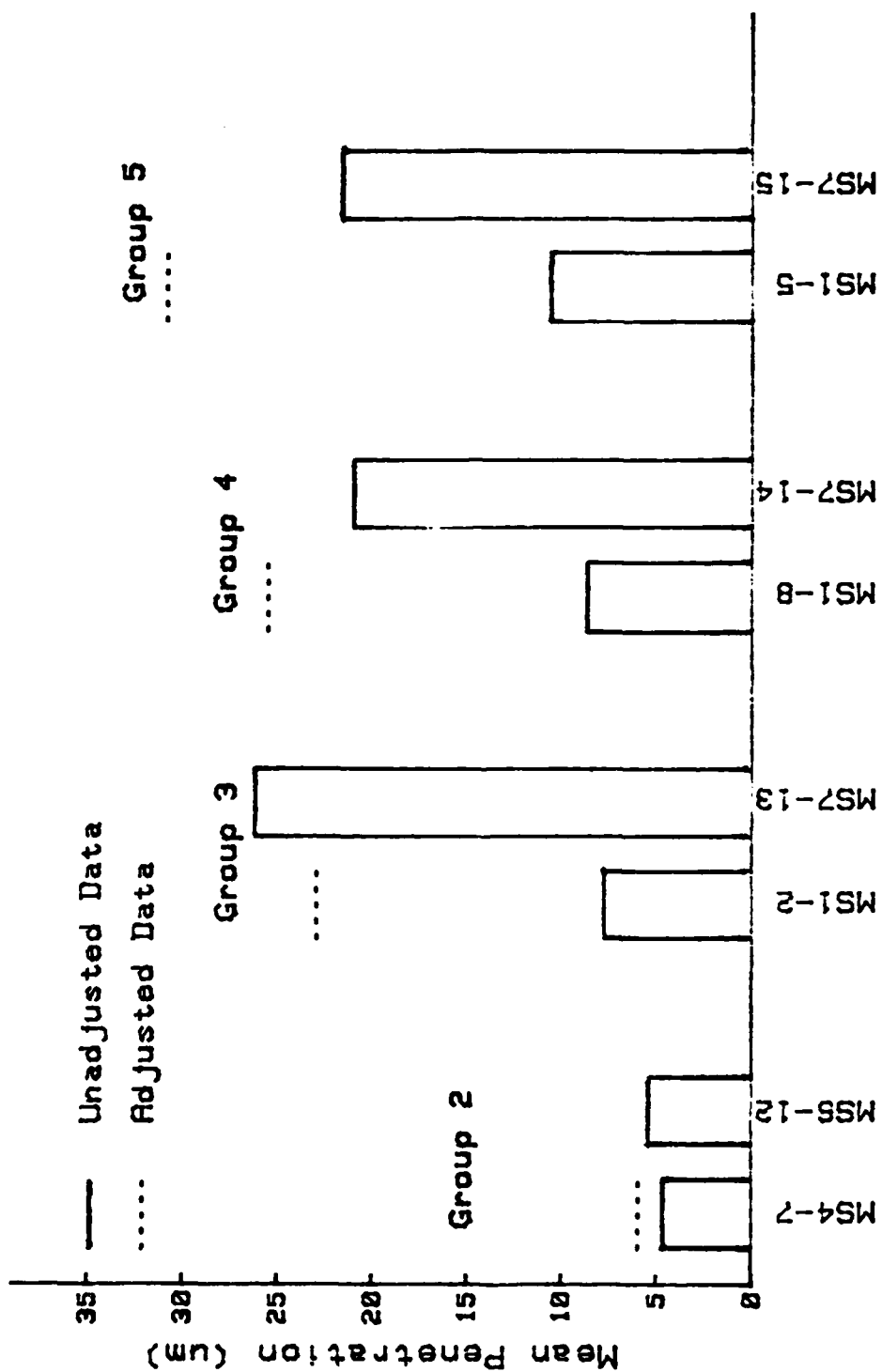


Figure B.9 Schematic Illustration of the Method of Using
High Magnification Spectrochemical Analysis for
Diffusion Study



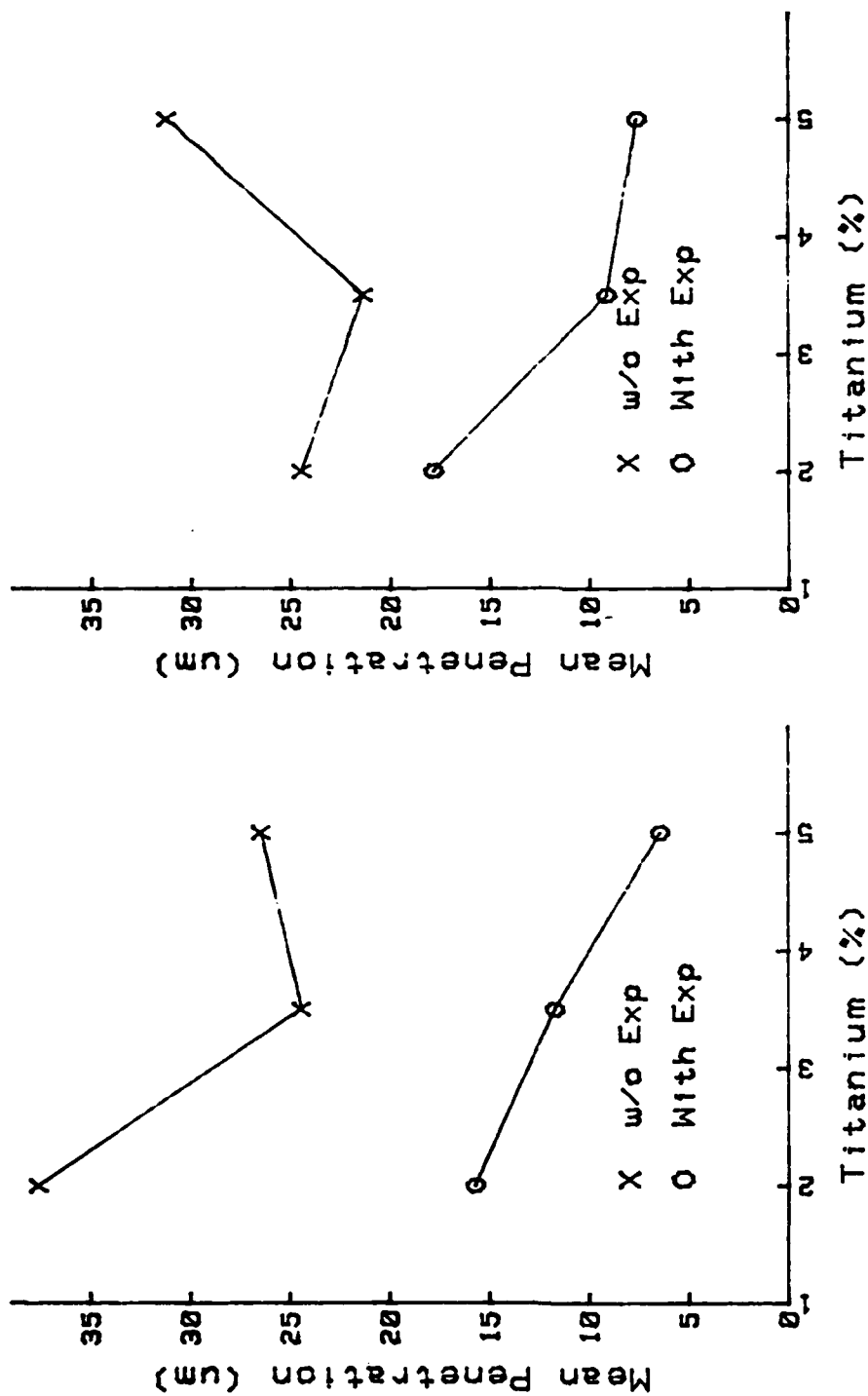
a) Control Pin Group 1

Figure B.10 The Effect of SO_2 Flow Rate on Type 2 Hot Corrosion of BC-21 Coated Rene' 80



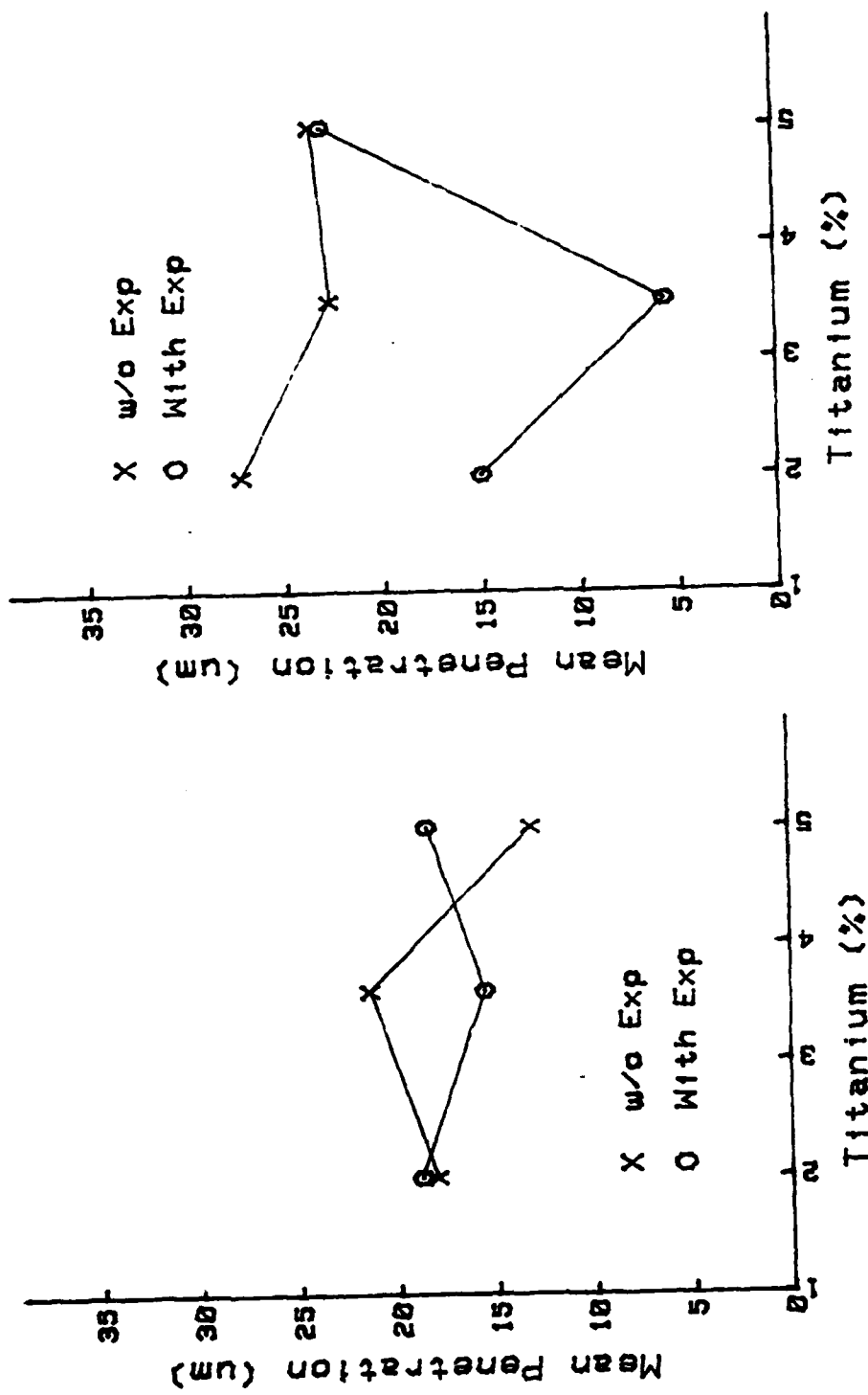
b) Control Pin Groups 2, 3, 4, 5

Figure B.10 (continued)



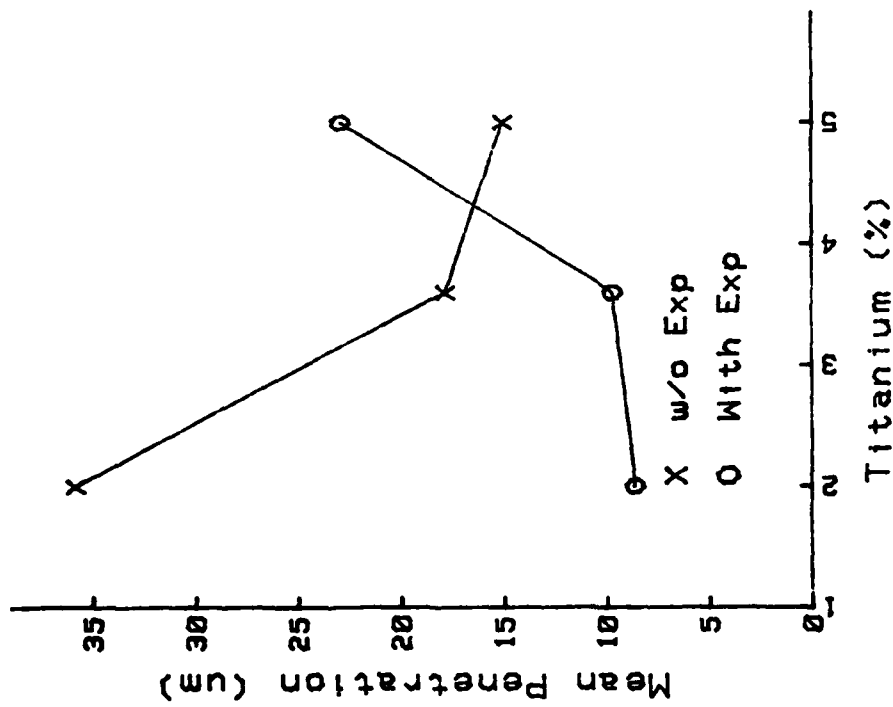
a) Without Pt Underlayer, without Hf Addition to Substrate
 b) Without Pt Underlayer, with Hf Addition to Substrate

Figure B.11 Type 2 Hot Corrosion Behavior of BC-21 Coated Rene' 80
 Modifications, Effect of Titanium

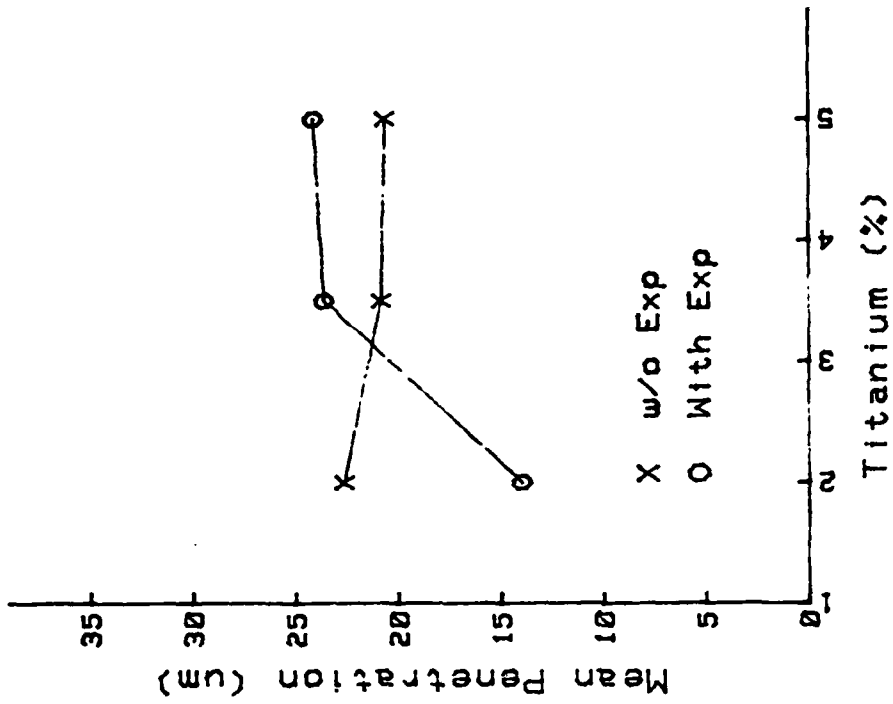


c) With Pt Flash Underlayer Without Hf Addition to Substrate
 d) With Pt Flash Underlayer With Hf Addition to Substrate

Figure B.11 (Continued)



e) With 5-6 μ m Pt Underlayer
Without Hf Addition to Substrate



f) With 5-6 μ m Pt Underlayer
With Hf Addition to Substrate

Figure B.11 (continued)

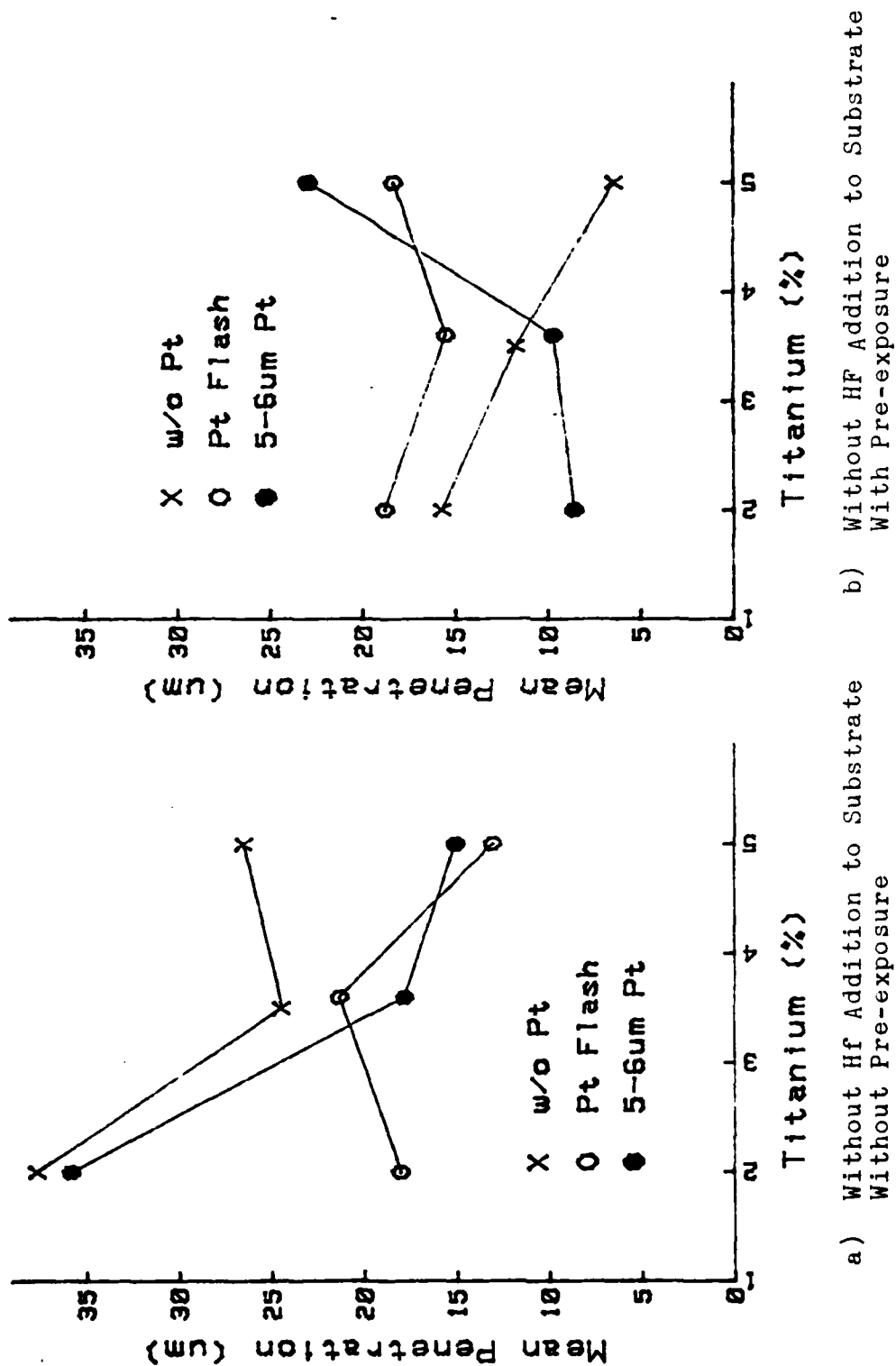
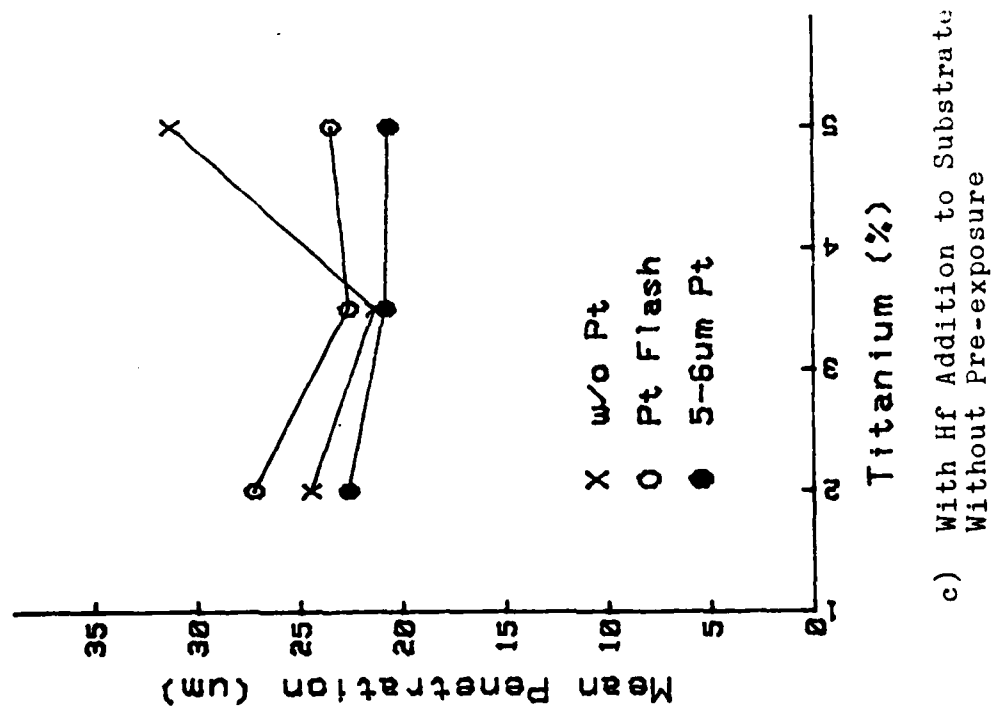
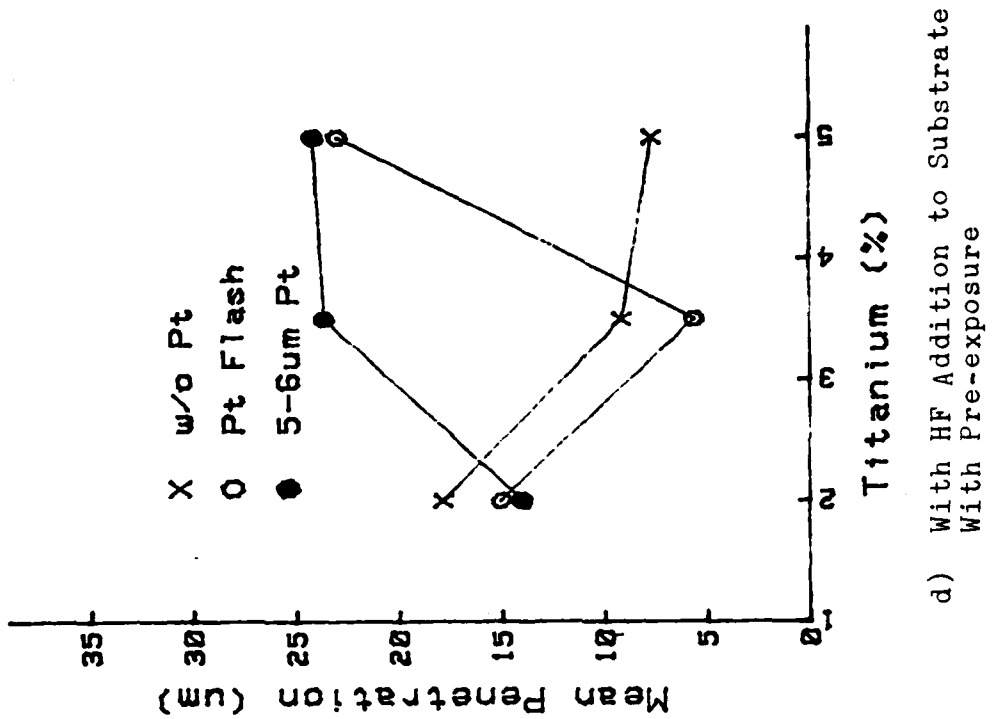


Figure B.12 Type 2 Hot Corrosion Behavior of BC-21 Coated Rene' 80
Modifications, Effect of Platinum



c) With Hf Addition to Substrate Without Pre-exposure



d) With HF Addition to Substrate With Pre-exposure

Figure R.12 (continued)

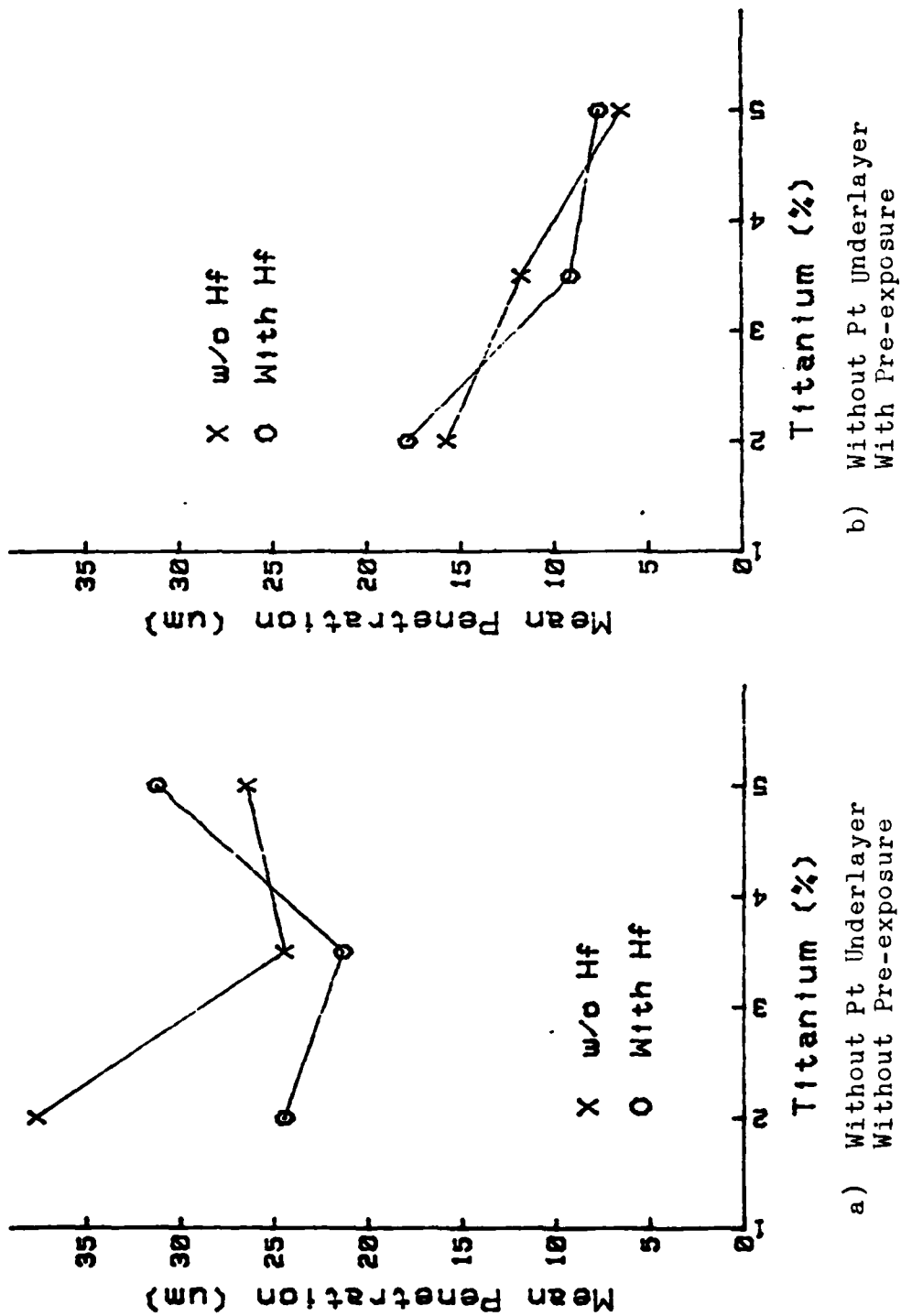
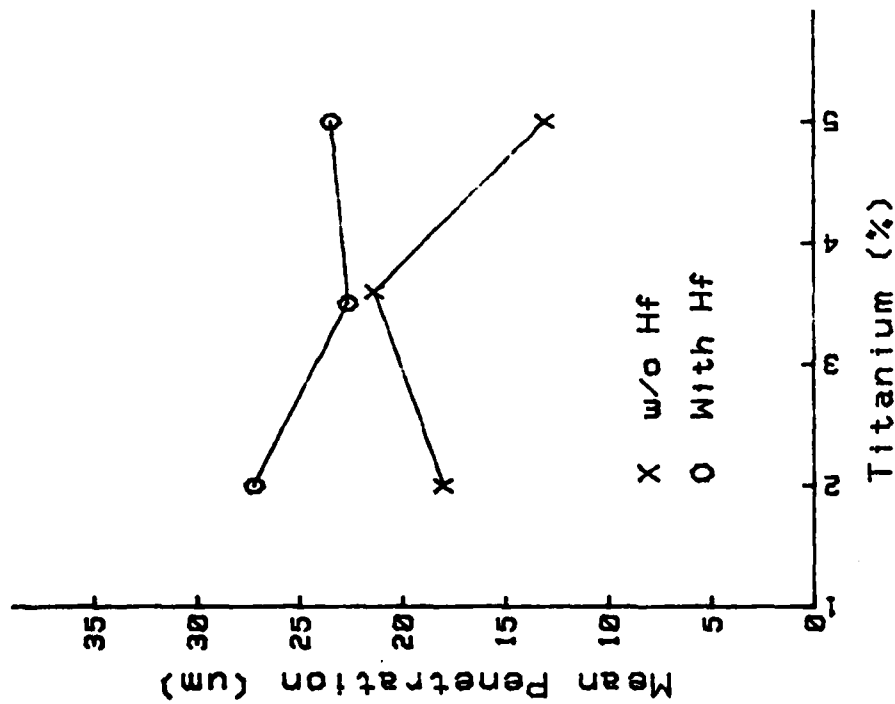
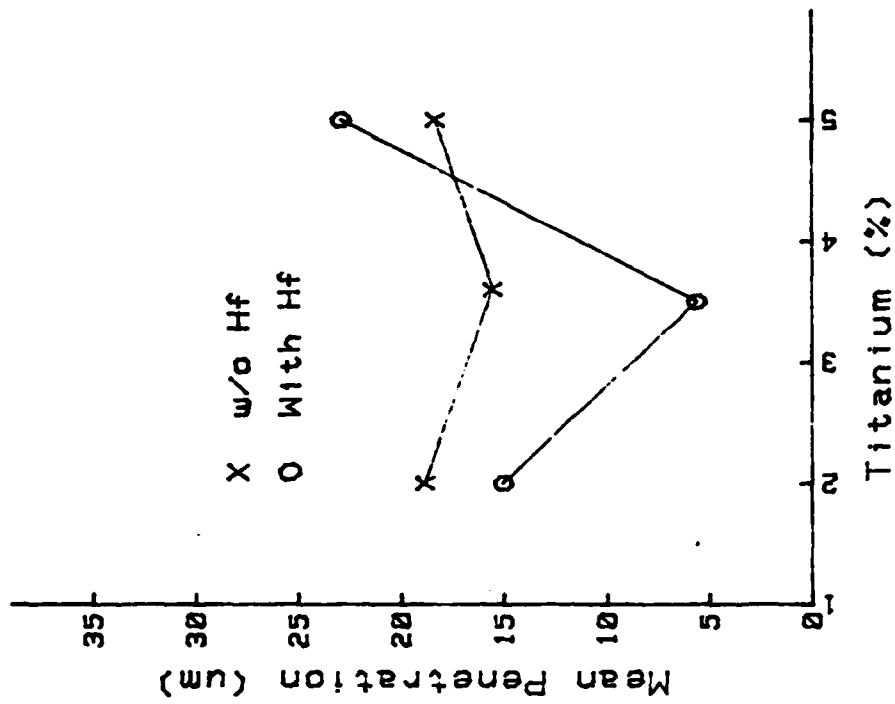


Figure B.13 Type 2 Hot Corrosion Behavior of BC-21 Coated Rene' 80
Modifications, Effect of Hafnium



c) With Pt Flash Underlayer Without Pre-exposure



d) With Pt Flash Underlayer With Pre-exposure

Figure B.13 (continued)

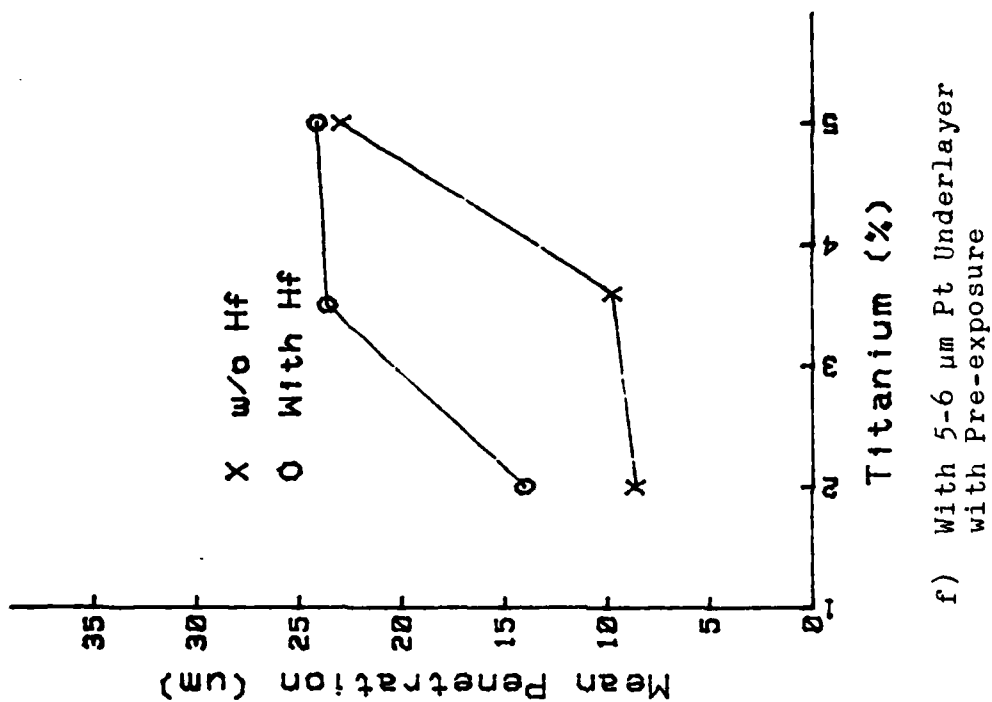
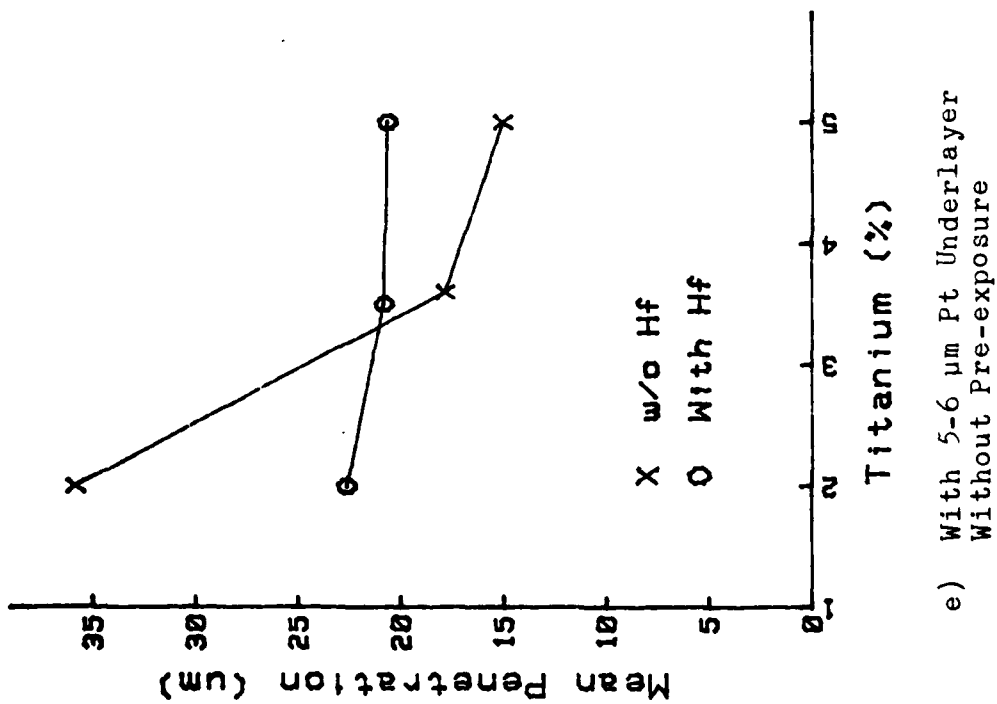
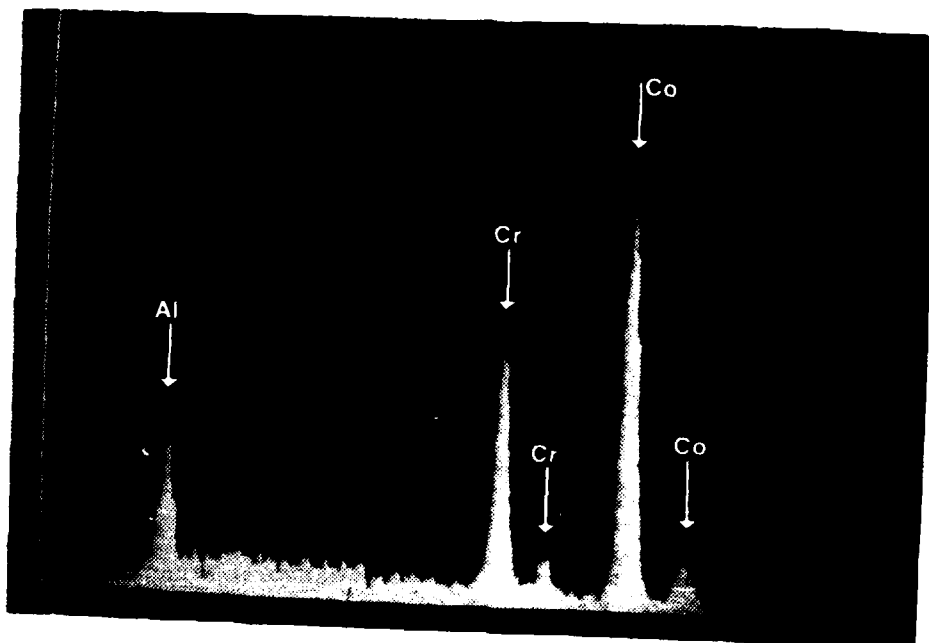
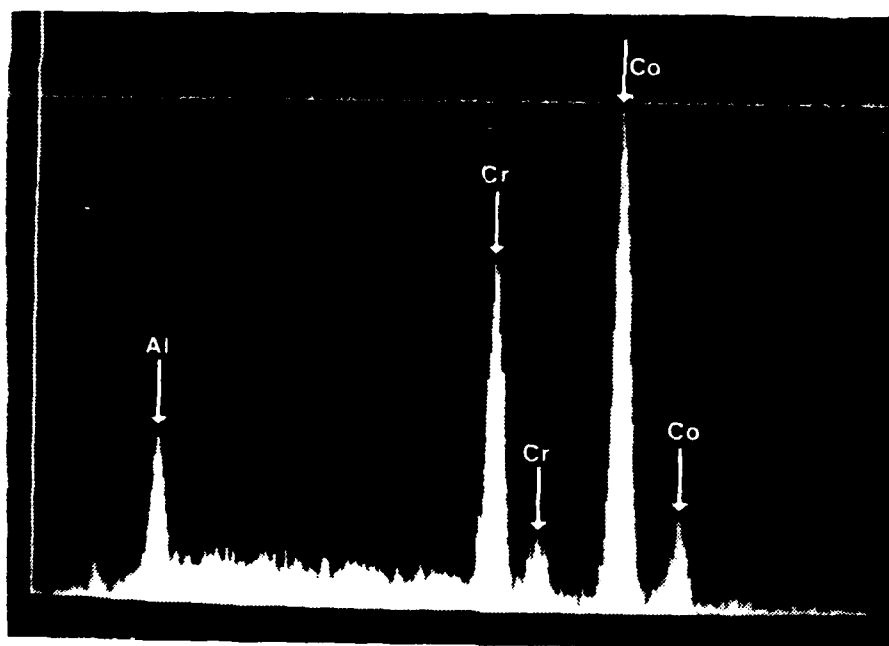


Figure B.13 (continued)

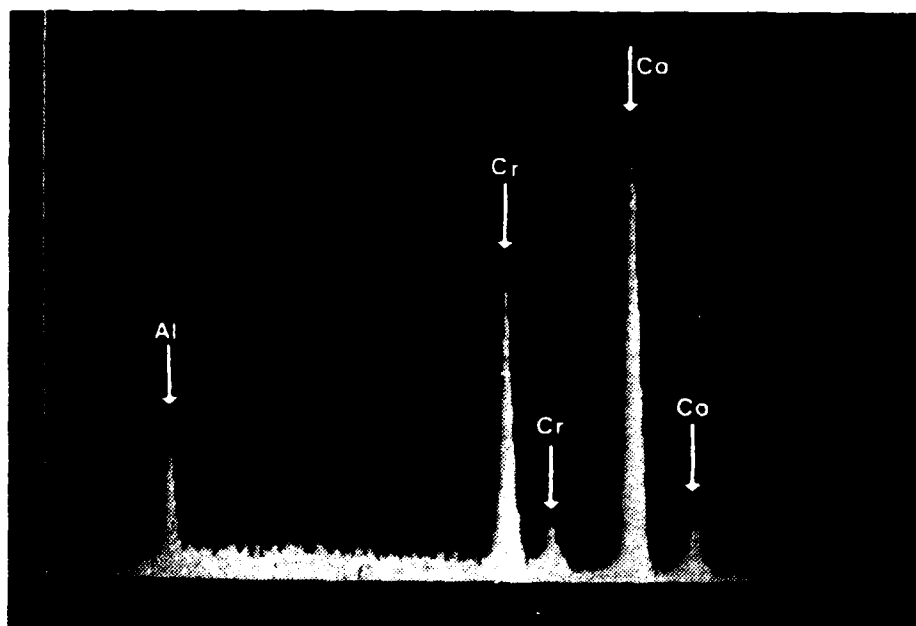


a) 5% Ti

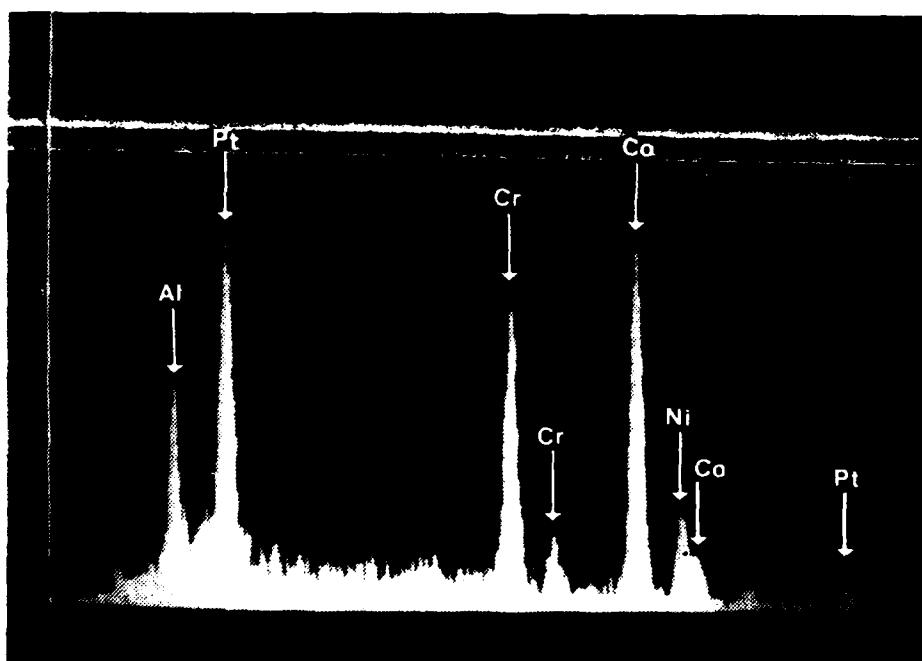


b) 5% Ti, with Pre-Exposure

Figure B.14 Chemical Spectrums of Center of B3-Al Coating on Corroded Rene' 30 (5% Ti Modification)



a) ^{53}Ti , 5 - 6 μm Pt.



b) ^{53}Ti , 5-6 μm Pt, with Pre-Exposure

Figure B.15 Chemical Spectrums of BC-21 Coating on Corroded
Rene' 80 (^{53}Ti Modification) with Platinum
Underlayer

LIST OF REFERENCES

1. Hawkins, P.F., "LM 2500 Operating Experience on GTS CALLAGHAN, " Proceedings of the 4th Conference on Gas Turbine Materials in a Marine Environment, pp. 39-69, Annapolis, MD, June 1979.
2. Boyer, H.E., ed., Metals Handbook, V. 10, American Society for Metals, 1975.
3. Brick, R.M., Gordon, R.B., and Pence, A.W., Structure and Properties of Engineering Materials, pp. 387-390, McGraw-Hill, 1977.
4. Jaffee, R.I., National Materials Advisory Board, Report NMAB-260, Hot Corrosion in Gas Turbines, May 1970.
5. Fontana, M.G., and Green, N.D., Corrosion Engineering pp. 361-367, McGraw-Hill, 1978.
6. Sims, C.T. and Hagel, W.C., eds., The Superalloys, Wiley, 1972.
7. King, R.N., An Investigation of the Substrate/Platinum Effect in Low Temperature Hot Corrosion of Marine Gas Turbine Materials, Master's Thesis, Naval Postgraduate School, June 1981.
8. Aprigliano, L.F., David W. Taylor Naval Ship Research and Development Center Report TM 28-78/218, Low Temperature (1300°F) Burner Rig Test of MCrAlY Composition Variations, September 26, 1978.
9. Fairbanks, J., "Ceramic Coating Development, A Technical Management Perspective," Proceedings of the 4th Conference on Gas Turbine Materials in a Marine Environment, pp. 749-764, Annapolis, MD, June 1979.
10. Jones, R.L., Naval Research Laboratory Memorandum Report 4072, A Summary and Review of NAVSEA Funded Low Power Hot Corrosion Studies, Washington, D.C., September 24, 1979.
11. Jones, R.L., Naval Research Laboratory Memorandum Report 5070, Hot Corrosion in Gas Turbines, Washington D.C., April 27, 1983.
12. Luthra, K.L., and Shores, D.A., "Morphology of Na_2SO_4 Induced Hot Corrosion at 600-750°C" Proceedings of the 4th Conference on Gas Turbine Materials in a Marine Environment, pp. 525-542, Annapolis, MD, June 1979.

13. Busch, D.E., The Platinum Effect in the Reduction of Low Temperature Hot Corrosion on Marine Gas Turbine Materials, Master's Thesis, Naval Postgraduate School, December 1980.
14. Collins, J.G., The Substrate Effect in Low Temperature Hot Corrosion of Marine Gas Turbine Coating Materials, Master's Thesis, Naval Postgraduate School, December 1981.
15. Exell, J.R., The Substrate Effect of Active Element Hafnium in Aluminide Coatings, Master's Thesis, Naval Postgraduate School, June 1981.
16. Newberry, G.D., Studies of Low Temperature Hot Corrosion of Uncoated Superalloys, Master's Thesis, Naval Postgraduate School, September 1981.
17. Jurey, S. N., Substrate Effects on Hot Corrosion Resistance of Nickel Base Superalloys, Master's Thesis, Naval Postgraduate School, June 1982.
18. McGowen, T.L., Type 1 Hot Corrosion Furnace Testing and Evaluation, Master's Thesis, Naval Postgraduate School, Monterey, California, October 1982.
19. Katz, G.B., and Boone, D.H., Lawrence Berkely Laboratory, University of California, Berkely, California Private Communication.
20. Clark, R.L., "Low and High Temperature (704°C and 899°C) Burner Rig Evaluations of Advanced MCrAlY Coating Systems," Proceedings of the 4th Conference on Gas Turbine Materials in a Marine Environment, pp. 189-220, Annapolis, MD, June 1979.

INITIAL DISTRIBUTION LIST

| | No. Copies |
|--|------------|
| 1. Defense Technical Information Center Cameron Station Alexandria, Virginia 22314 | 2 |
| 2. Library, Code 0142 Naval Postgraduate School Monterey, California 93940 | 2 |
| 3. Department Chairman, Code 69 Department of Mechanical Engineering Naval Postgraduate School Monterey, California 93940 | 1 |
| 4. Adjunct Professor D. E. Peacock, Code 69 Department of Mechanical Engineering Naval Postgraduate School Monterey, California 93940 | 2 |
| 5. Adjunct Professor D. H. Boone, Code 69bi Department of Mechanical Engineering Naval Postgraduate School Monterey, California 93940 | 6 |
| 6. Mr. Louis F. Aprigliano, Code 2812 David W. Taylor Naval Research and Development Center Annapolis, Maryland 21402 | 2 |
| 7. LT Michael J. Shimko 6409 Fair Oaks Avenue Baltimore, Maryland 21218 | 2 |

**DAT
ILM**